ESA-MOST Dragon Cooperation

中国科技部-欧洲空间局“龙计划”合作

2017 DRAGON 4 SYMPOSIUM

2017年“龙计划”四期学术研讨会

Project: Monitoring Cryosphere Dynamic over HMA with Integrated Earth observations and Evaluating Its Hydrological Impacts at Upstrem River Basin (32388)

Lin Hui (The Chinese University of Hong Kong), Andrew Hooper (The University of Leeds)

Pis: Jiang Liming (WHIGG, CAS), Lan Cuo (ITPCAS), Meng Liqiu (TUM)

26–30 June 2017 | Copenhagen, Denmark

2017年6月26-30日，丹麦 哥本哈根

A DECREASING GLACIER MASS BALANCE GRADIENT FROM THE EDGE OF THE UPPER TARIM BASIN TO THE KARAKORAM EAST DURING 2000-2013

Gang Li, Hui Lin, Lan Cuo, Andrew Hooper, Liming Jiang, Qinghua Ye, Lin Liu

Decadal glacier mass balance for Western Nyainqêntanglha and its melting contribution to Nam Co's increasing

Most Tibetan Plateau Lakes experienced sharp increasing during 2003 and 2009 by satellite altimetry (Zhang et al., 2011RSE).

Previous researches believe glaciers degradation is should be responsible (Yao et al., 2007; Yao et al., 2010; Zhu et al., 2010), but recent analyzes by GRACE and hydrological model analyze suggest precipitation contribute almost all water volume increasing, except Nam Co Lake (Zhang et al., 2013GRL; Lei et al., 2013JHydro).

According to in-situ observation at Zhadang Glacier (-0.59m/a) and hydrological model, 28.7% of Nam Co Lake increasing are contribute by glaciers' melting at northern slope of Western Nyainqêntangla (Lei et al.,2013).

Second largest lake in Tibetan Plateau.

Highest endorheic lake in the world.

Area: 2021.3 km^2 Catchment Area: 10740 km^2 Glacier area (Inside Nam Co Basin): 196.8 km^2 Increasing rate: 0.25 $\pm$ 0.12 m/yr (ICESat)

Decadal glacier mass balance for Western Nyainqêntanglha and its melting contribution to Nam Co's increasing

Methods:

Five bitatic TSX/TDX images in COSSC format are process for deriving decadal glacier height changes respect to SRTM.

Penetration depth evaluated by comparing C and X band SRTM.

Given the short distance from glacier terminus to Nam Co, all melting are supposed to flow into Nam Co Lake following Lei Yanbing's research.

Acquisition date	Perpendicular Baseline (m)	Pass	Incidence angle
2013-03-30	376	A	46
2012-12-02	-145	D	34
2014-03-12	146	A	34
2014-03-23	164	A	36
2014-04-07	-163	D	46

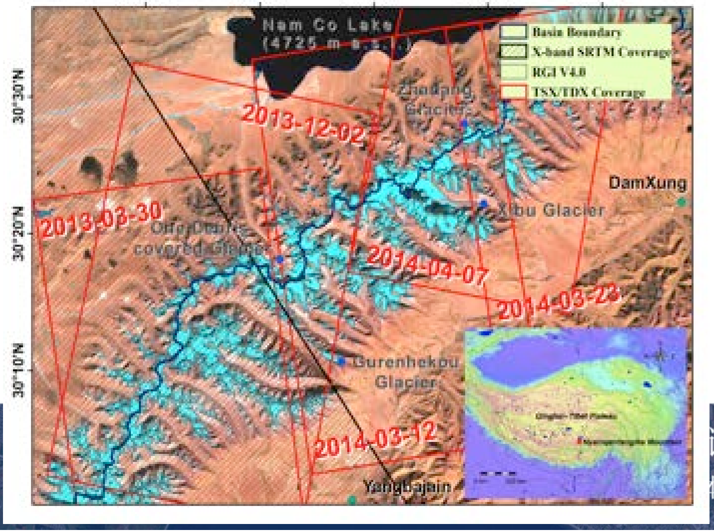

Decadal glacier mass balance for Western Nyainqêntanglha and its melting contribution to Nam Co's increasing

Area	Glacier Height Changes in 14 Years (m)	Glacier Mass balance rate (w.e. m yr^{-1})
Western NyQ Mt	- 3.822 ± 0.552	- 0.235 ± 0.127
In Nam Co Basin	- 4.408 ± 0.562	- 0.268 ± 0.129
Out Nam Co Basin	- 3.610 ± 0.551	- 0.219 ± 0.126

Slight glacier mass balance differences at northern and southern slope mainly due to their height distribution difference.

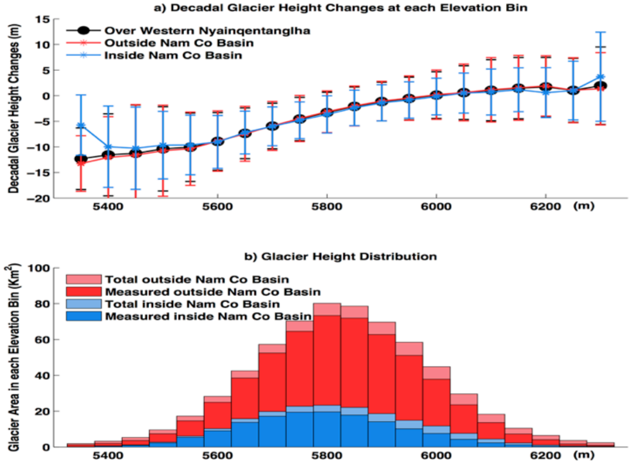

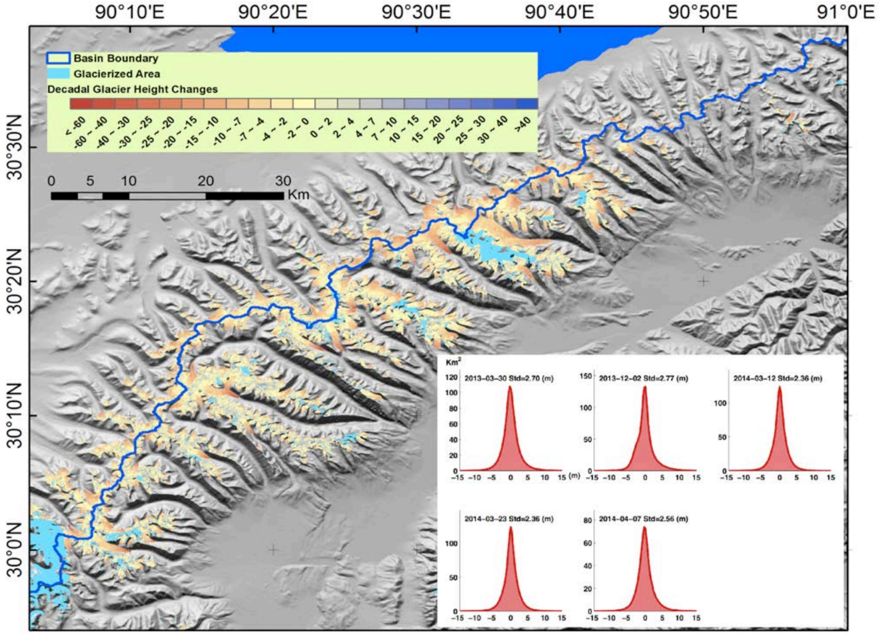

Decadal glacier mass balance for Western Nyainqêntanglha and its melting contribution to Nam Co's increasing

Validation to in-situ observation

Name	ZMIN/ZMED/ZMAX (a.s.l m)	Area (km²)	in-situ mass balance (m w.e. yr⁻¹)	mass balance (m w.e. yr⁻¹)
Zhadang	5512/5751/6079	2.912	- 0.59	- 0.501± 0.166
Gurenhekou	5489/5779/5979	1.574	- 0.31	-0.267 ± 0.248

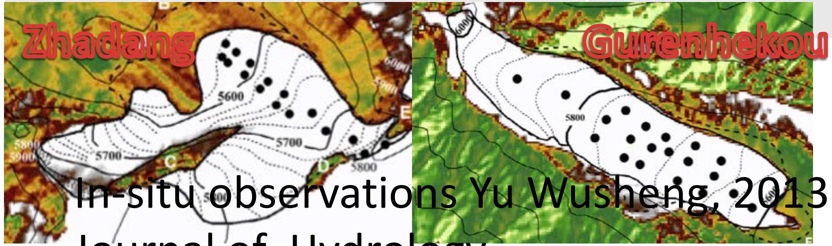

In-situ observations Yu Wusheng, 2013 Journal of Hydrology

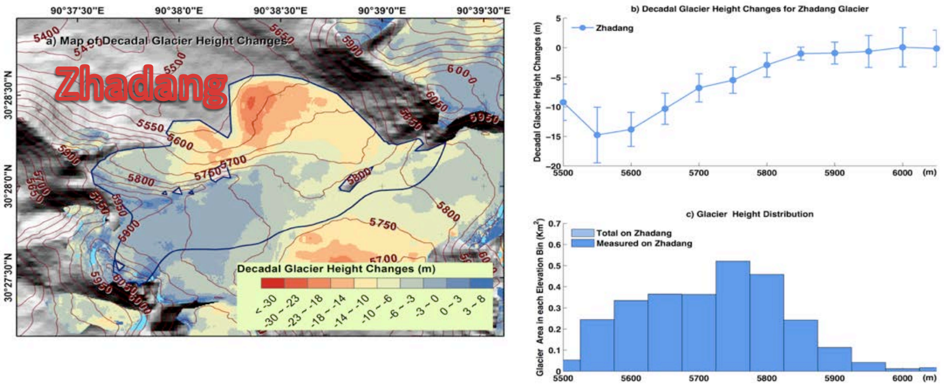

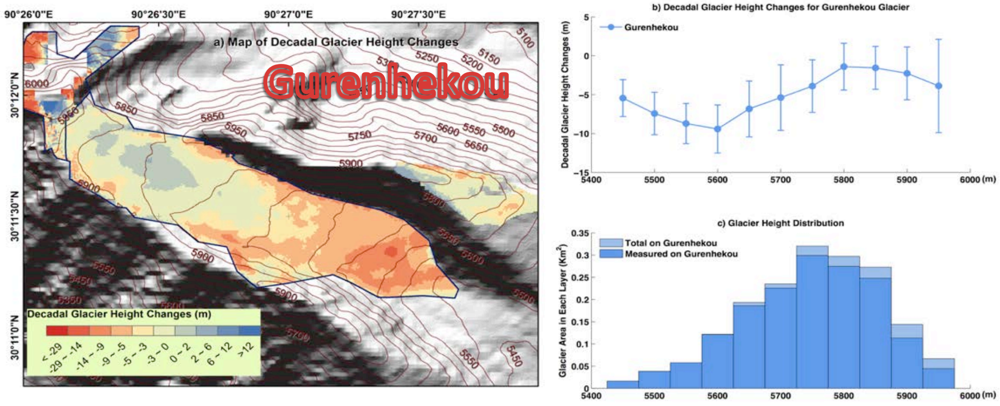

Decadal glacier mass balance for Western Nyainqêntanglha and its melting contribution to Nam Co's increasing

Glacier mass balance in the first decade of the 21st century was -0.235 ± 0.127 m w.e. yr^{-1} for the Western Nyainqentanglha Mountains glaciers.

If glacier melt was assumed to flow into the Nam Co Lake without any evaporation, it contributed 10.50 ± 9.00 % to the Nam Co Lake volume increase between 2003 and 2009, which is considerably less than was observed in previous studies.

Ref to: Li, G., Lin, H. (2017) Recent decadal glacier mass balances over the Western Nyainqentanglha Mountains and the increase in their melting contribution to nam co lake measured by differential bistatic SAR interferometry. Global and Planetary Change, 149, 177-190.

A decreasing glacier mass balance gradient from the edge of Upper Tarim Basin to Karakoram during 2000-2014

In contrast to other sub-regions of the HMA that are experiencing glacier mass loss, including the Himalayas, Eastern Nyainqentanglha, Spiti Lahaul and Tien Shan, the Pamir-Karakoram-Kunlun region includes glaciers that have gained mass, although the details are debated (Gardelle 2012 & 2013; Kääb 2012 & 2015; Farinotti 2015).

For the Karakoram to the western Pamir, a positive mass balance was suggested from comparing DEMs from the SRTM, and stereo photogrammetry-formed DEMs from 2012 SPOT/HRS data. This was termed as ‘Karakoram anomaly’ (Gardelle et al., 2012) and later the ‘Karakoram-Pamir anomaly’ (Gardelle et al., 2013). However, a satellite laser altimetry mission ICESat/GLAS indicated that a positive mass balance existed at the West Kunlun and Eastern Pamir, but stopped at the edge of the Karakoram with 1*1° gridding (Kääb et al., 2012 & 2015).

Zone	Kääb et al. 2015	Gardner et al. 2013	Neckel et al. 2014	Gardelle et al. 2013
Karakoram	-0.10 ± 0.06	-0.12 ± 0.15	-	+0.12±0.19
Hindu Kush	-0.49 ± 0.10	-	-	-0.14±0.19
Pamir	-0.48 ± 0.14	-0.13 ± 0.22	-	+0.16±0.15
West Kunlun	-0.05 ± 0.07	+0.17 ± 0.15	+0.04 ± 0.29	-

A decreasing glacier mass balance gradient from the edge of Upper Tarim Basin to Karakoram during 2000-2014

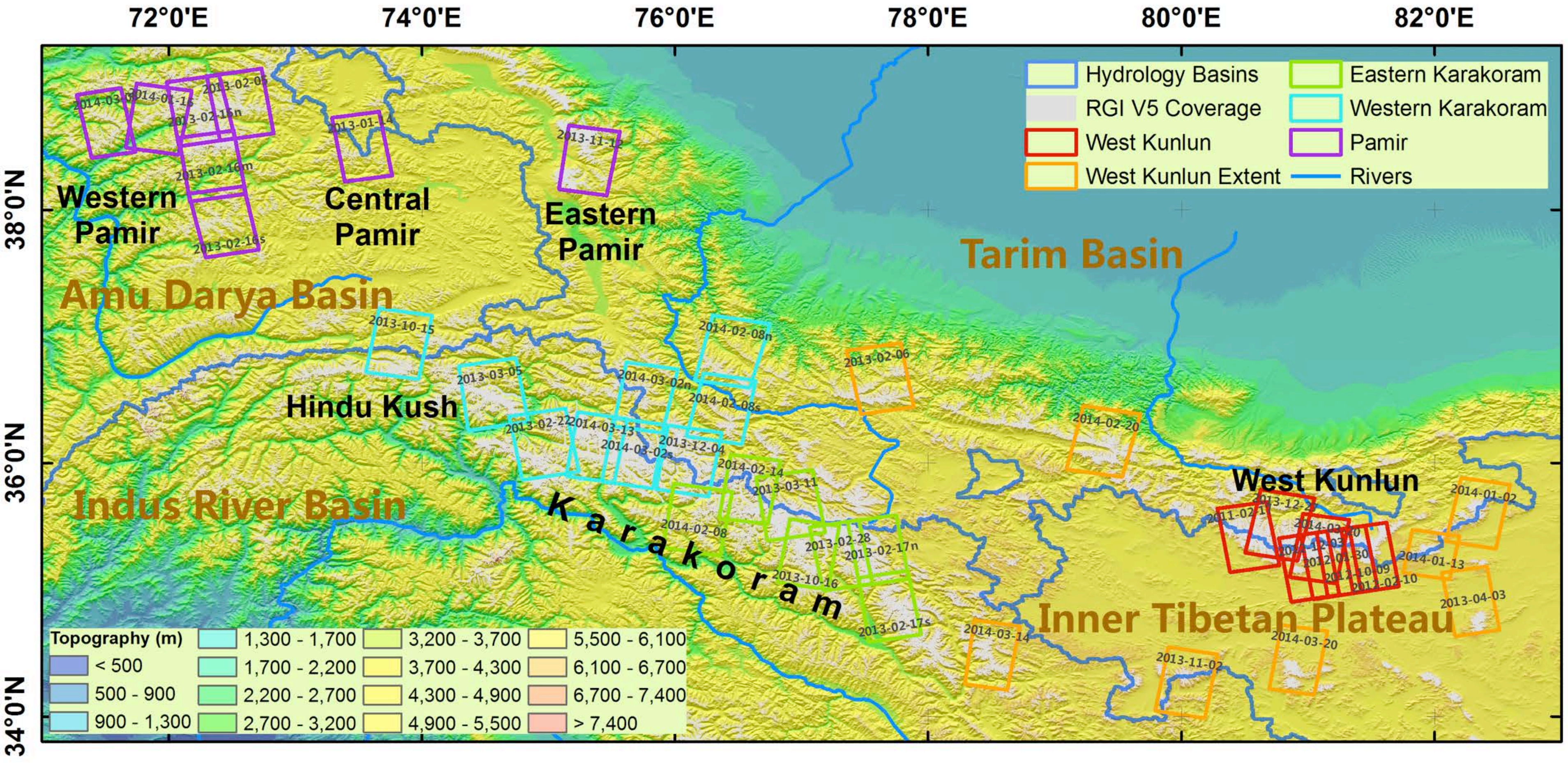

A decreasing glacier mass balance gradient from the edge of Upper Tarim Basin to Karakoram during 2000-2014

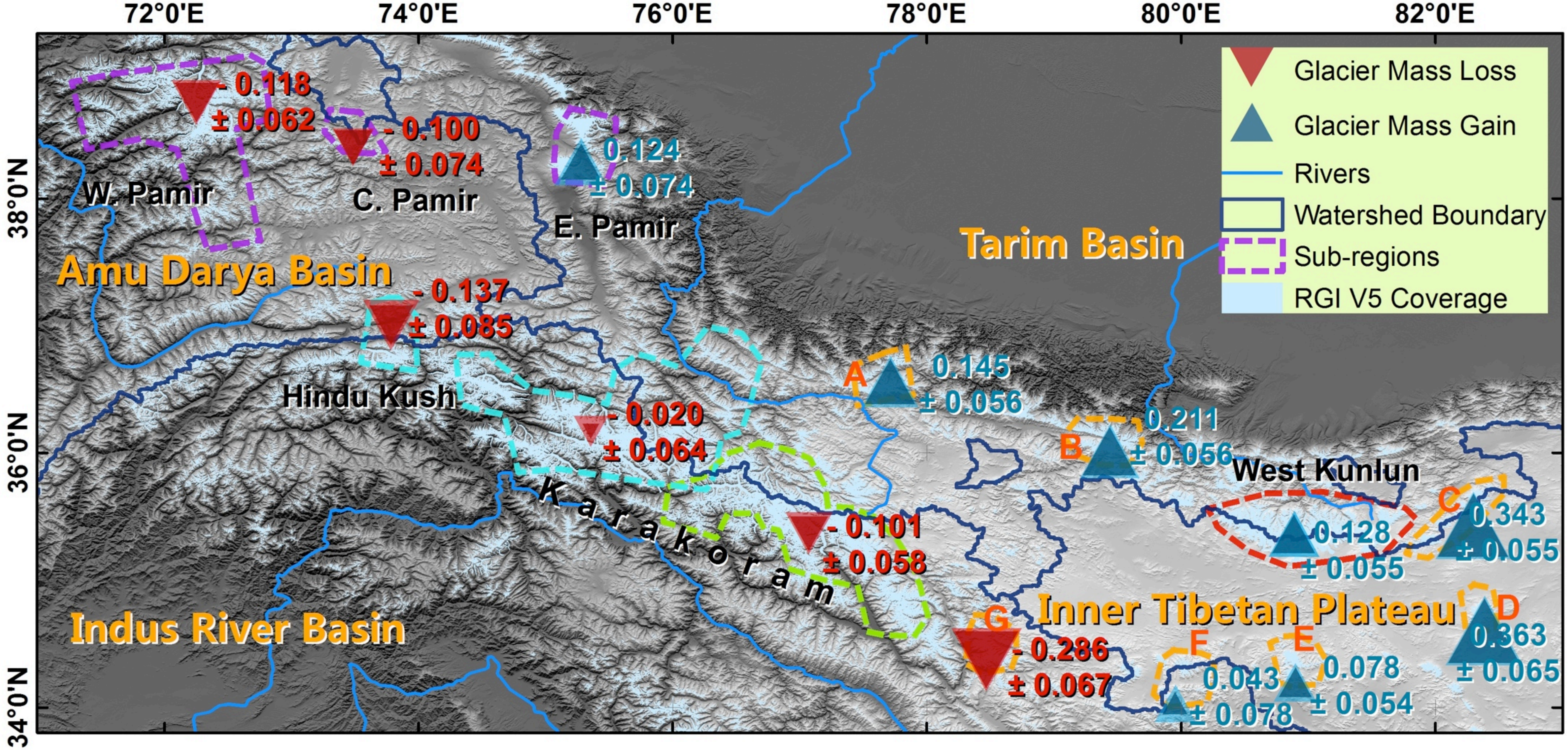

A decreasing glacier mass balance gradient from the edge of Upper Tarim Basin to Karakoram during 2000-2014

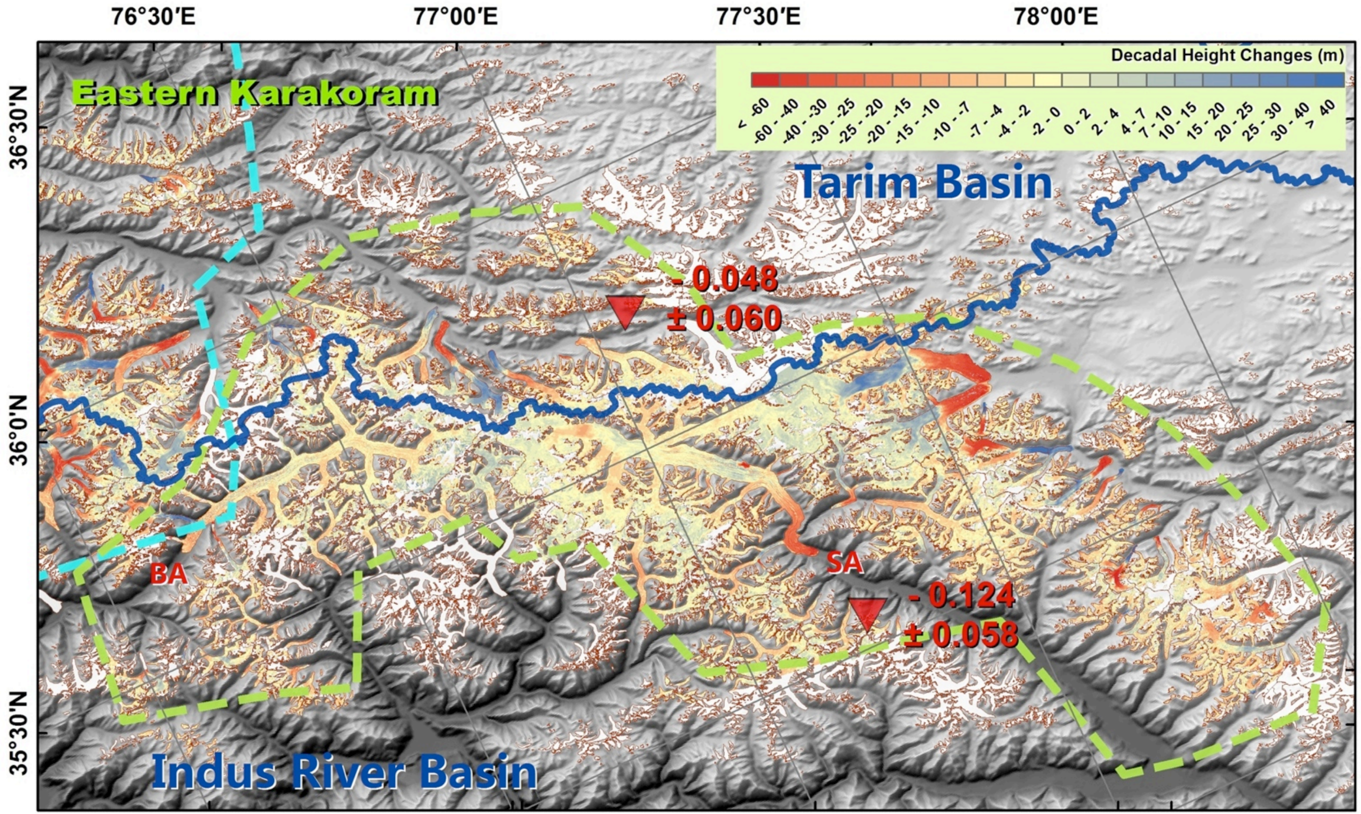

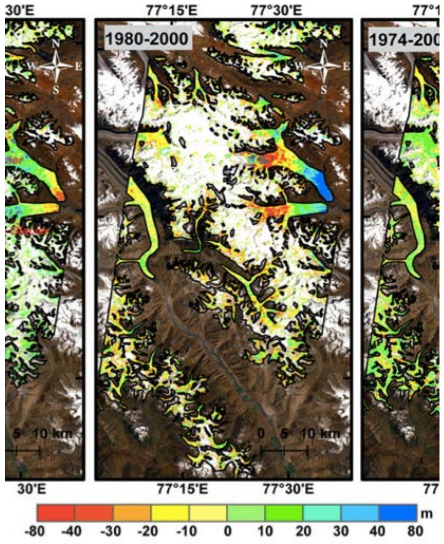

Zhou Yushan, et al., (2017 JoG)

Siachen Glacier. 72 Km, 1078 Km^2 Glacier mass balance: -0.08 ± 0.06 m w.e. a^{-1}

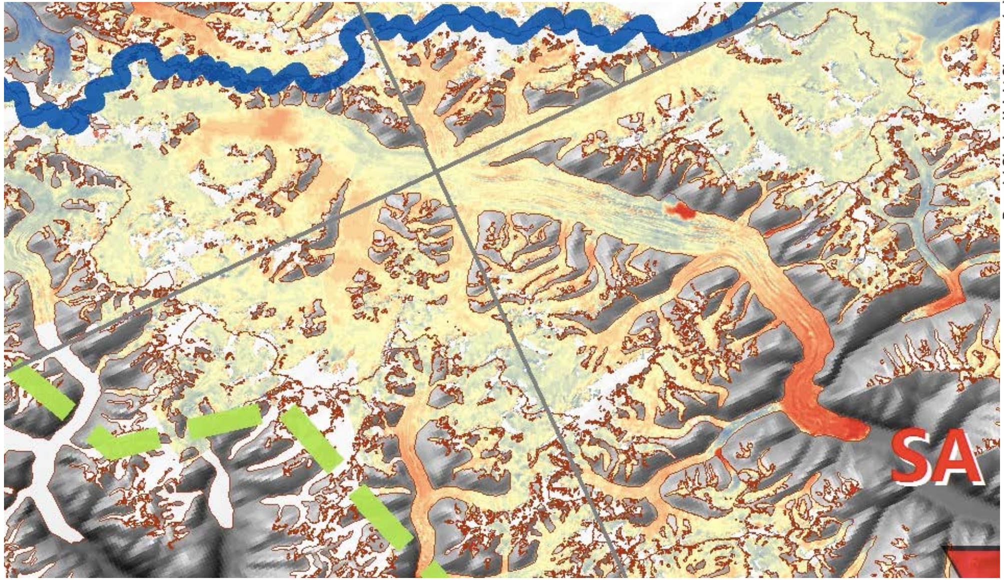

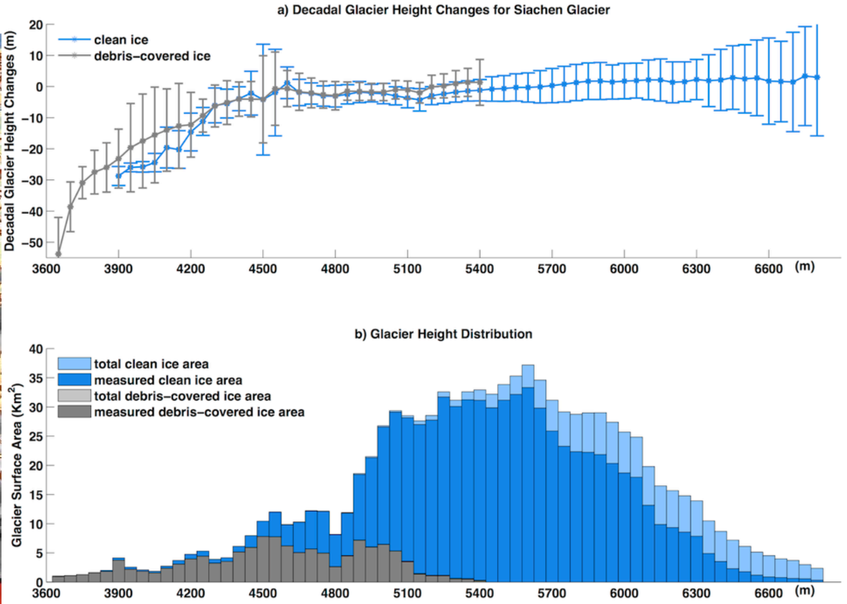

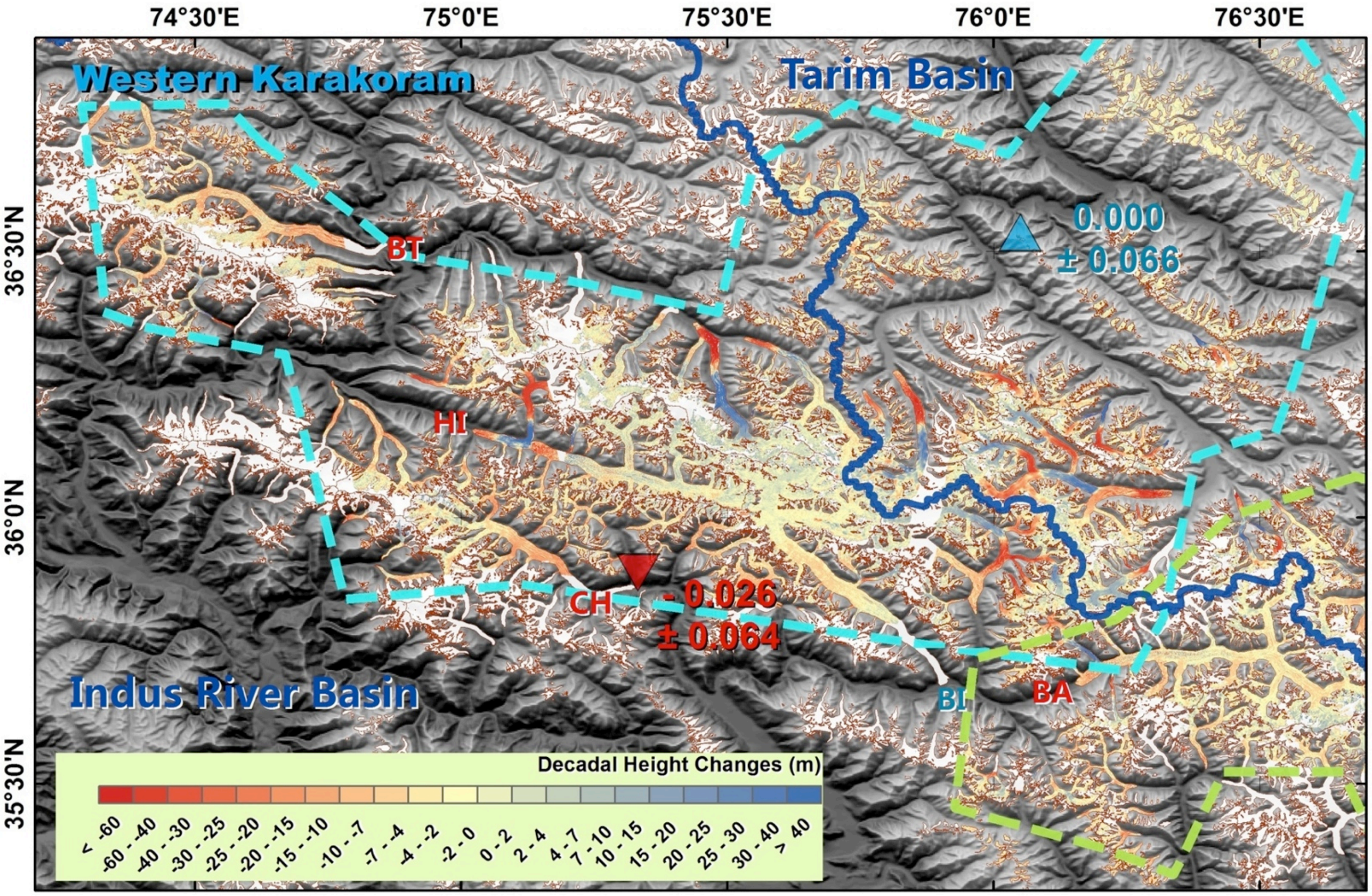

Western Karakoram

Most surging or stagnant glaciers are found inside Tarim Basin (northern slope).

At the most northeastern, glacier changes in every elevation bin is homogeneous.

Hindu Kush

Glaciers as Hindu Kush suffered from thinning. Surging glaciers are seldom found in this region.

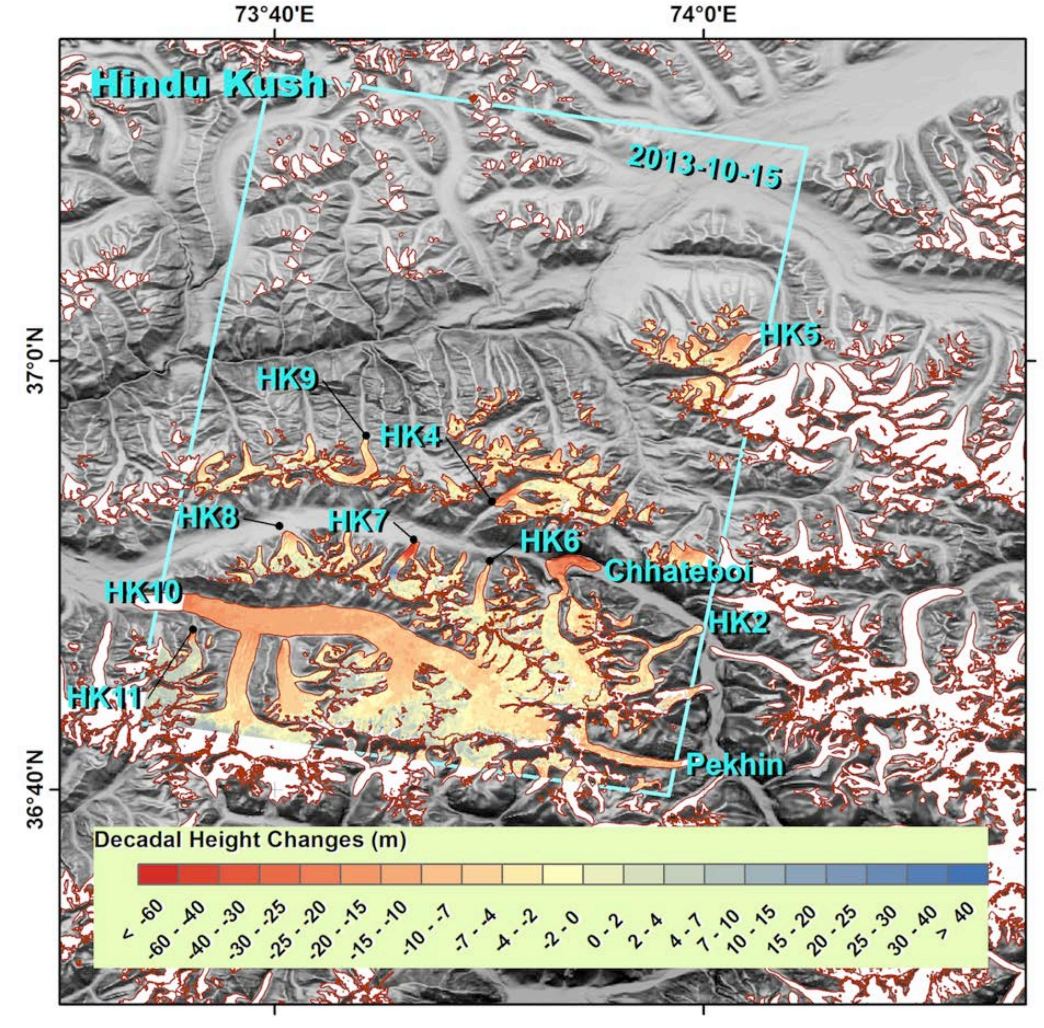

Western Pamir

Glaciers surging at west to Fedchenko is common, and their mass balance are stable. Glaciers in other regions downwasted significantly in ablation zone.

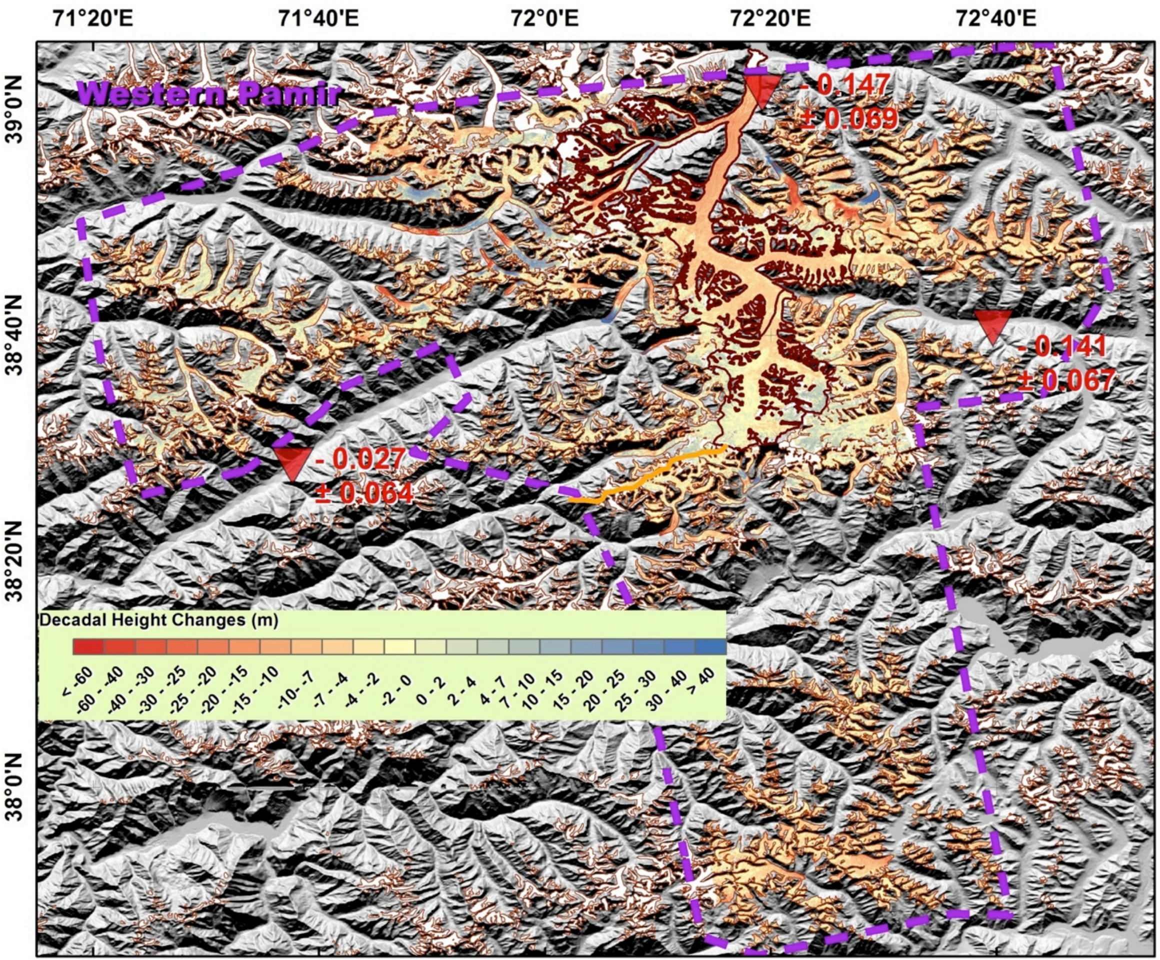

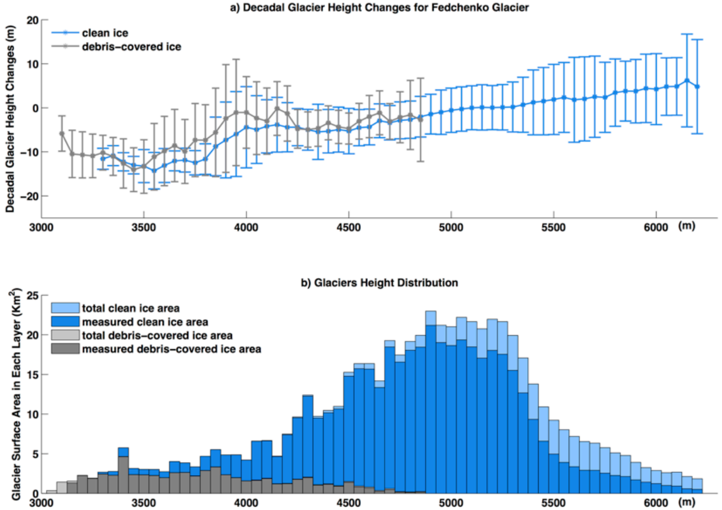

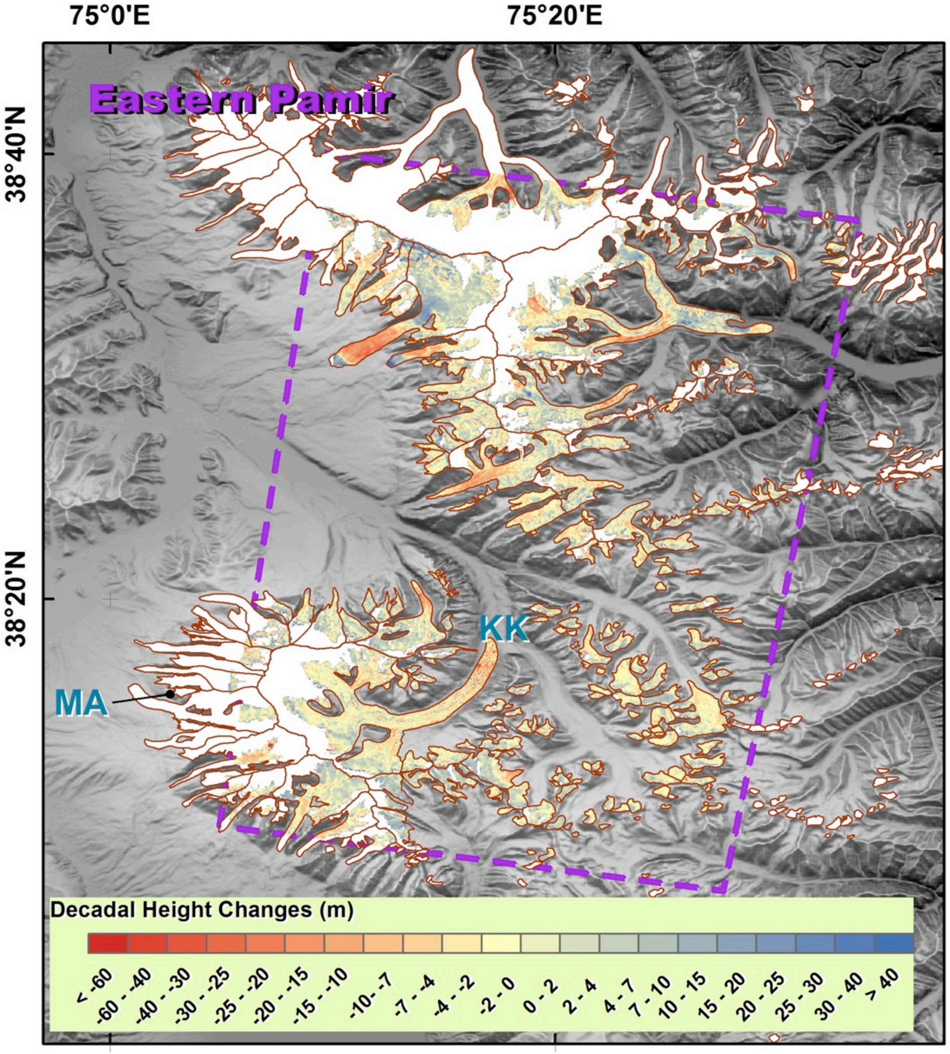

Eastern Pamir

The glacier height changes pattern is similar to Holzer et al.'s publication in The Cryosphere (2015).

However, due to large void area in SRTM dataset, great parts, especially in accumulation zone, were not observed.

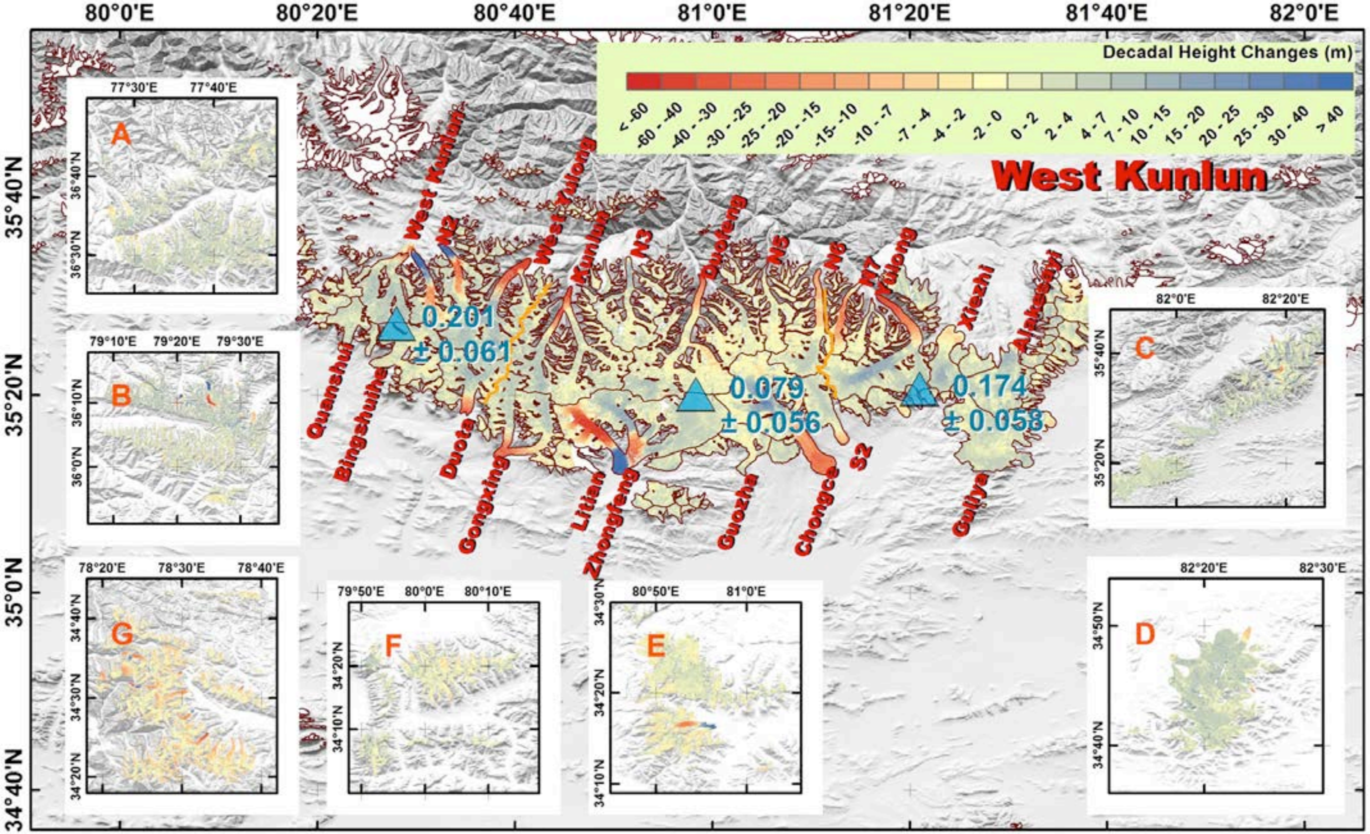

Region or sub-region	Mass balance in unit of w.e. yr^{-1}
West Kunlun (WK)	0.128±0.055
WK South (ITP)	0.095±0.057
WK North (Tarim)	0.144±0.057
WK East	0.174±0.058
WK Central	0.079±0.056
WK West	0.201±0.061

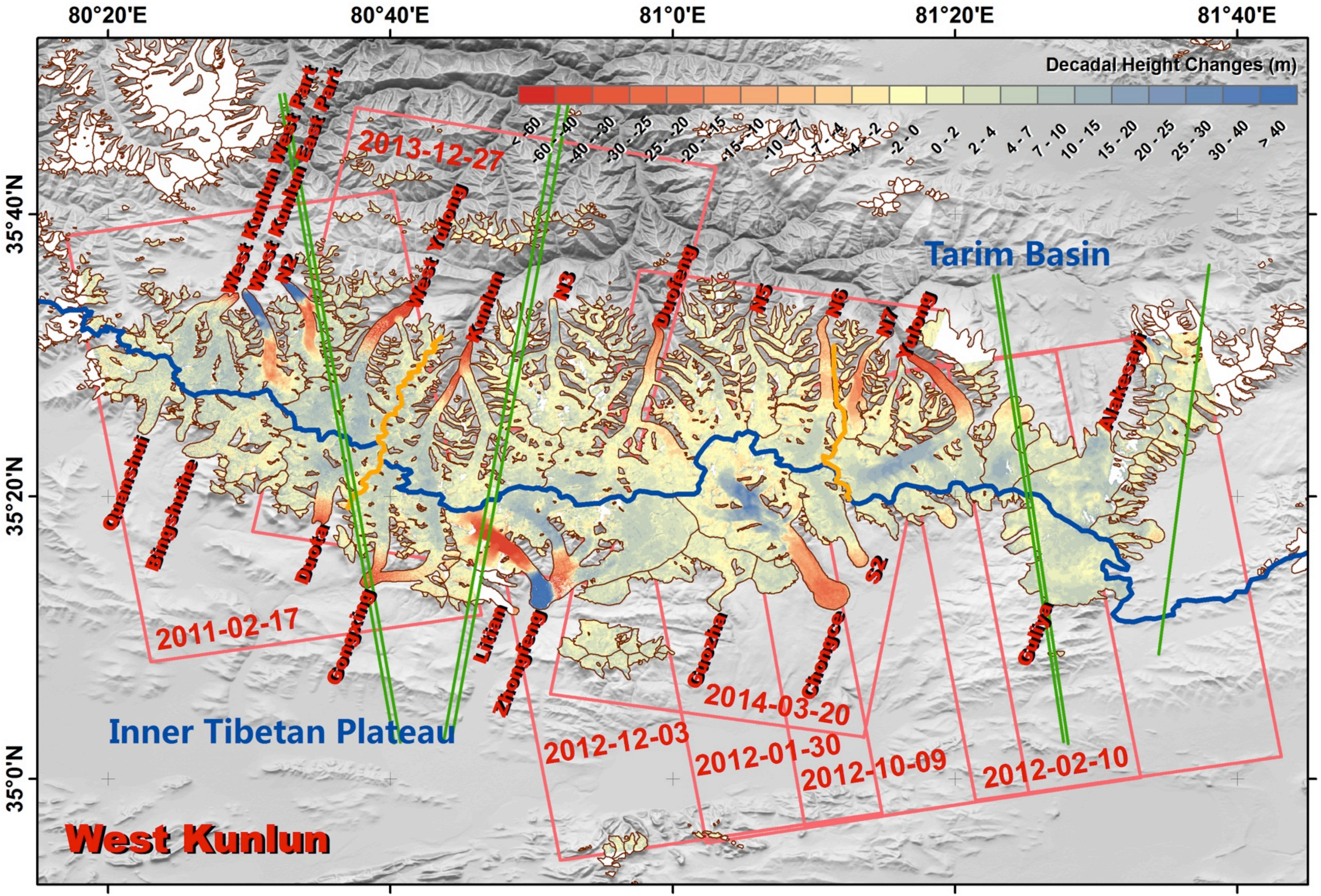

SurgeType：
West Kunlun,
N2, N7, Zhongfeng.

Stagnant,
West Yulong,
Duota, Gongxing,
Zhongfeng 2-4,
Chongce.

Yulong is the only one not detected by feature tracking

Yasuda, et al., 2013RSE

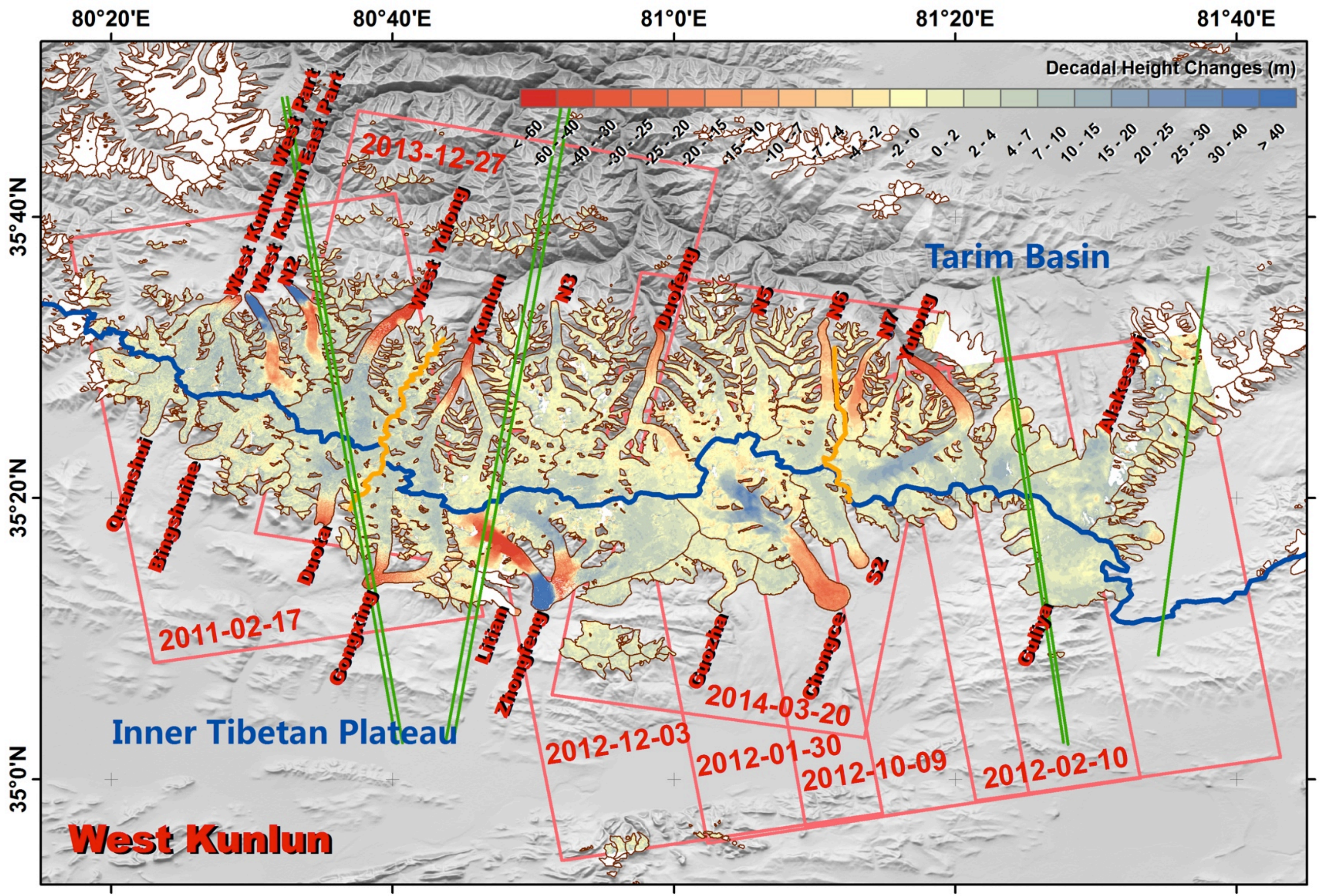

Compare to Ke et al., 2015RSE

Glacier Name	dH Trend (Ke's)	This study w.e.
West Yulong	0.34 ± 0.12	0.16 ± 0.07
Gongxing	-0.04 ± 0.23	0.16 ± 0.07
Zhongfeng	-1.15 ± 0.41	0.12 ± 0.07
Kunlun	0.13 ± 0.18	0.11 ± 0.07
Guliya	0.29 ± 0.09	0.23 ± 0.07

After removing all surged and stagnant glaciers, decadal glacier height changes were binned into every 50m elevation layers.

Above 5400m, glacier height changes are homogeneous in every elevation bin, while below such level, they downwasted dramatically.

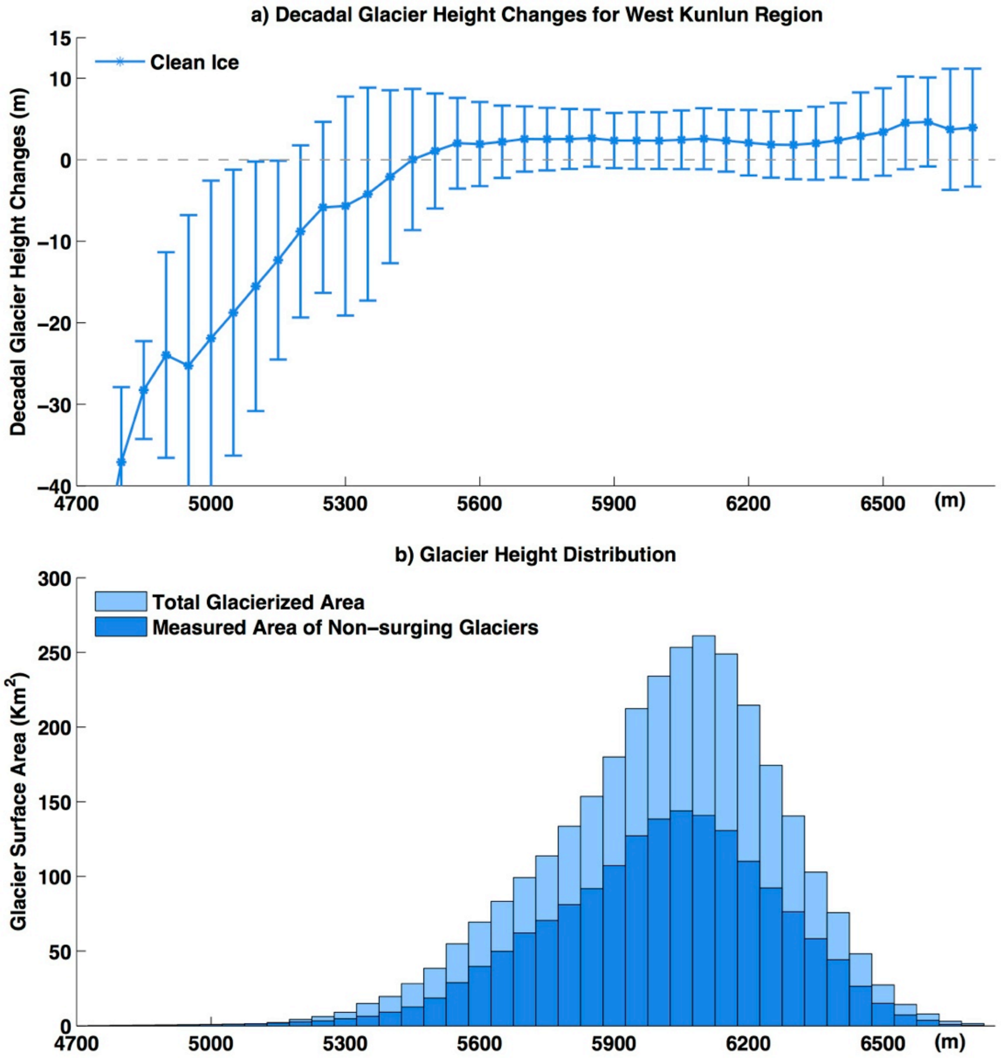

GCMs simulations do not show a strong mass balance anomaly along the edge of the Upper Tarim region; instead, they suggest that the major anomaly region occurs along 36.5N° in Western Karakoram (Janes, et al., 2012). In contrast, seven TSX/TDX images in our study region, covering the Hindu Kush region to the eastern extent of West Kunlun, show that the mass balance increases from west to the east (Fig. 8, Supplementary Fig. S1, S19 a b & c, S23, S27, S28, S29). This is similar to the finding using ICESat/GLAS observations along 36 N°.

Ref to: Lin, H., Li, G*., Lan, C., Hooper, A., Ye, Q. (2017) A decreasing glacier mass balance gradient from the edge of the Upper Tarim Basin to the Karakoram during 2000-2014. Scientific Reports. In press.

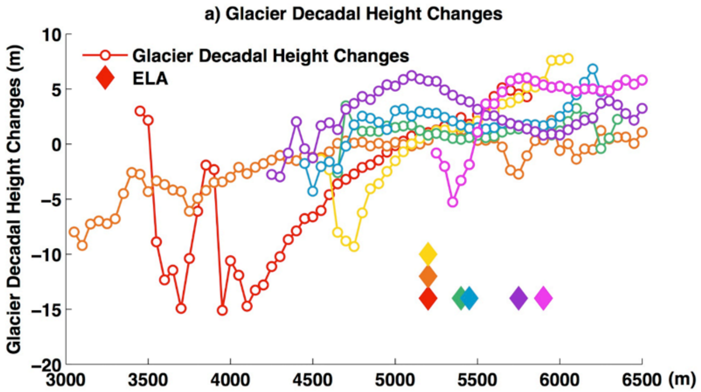

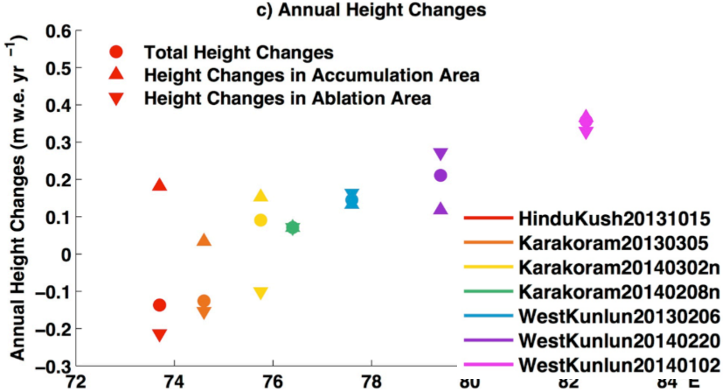

Kääb et al., 2015 The Cryosphere

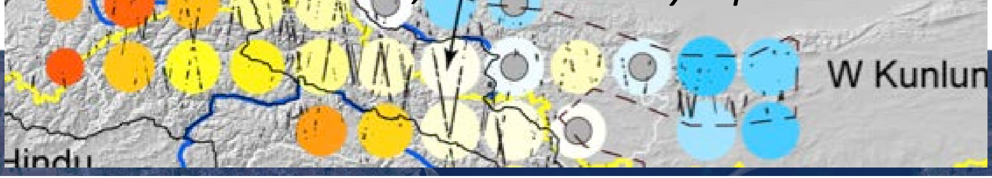

Heterogeneous pattern of glacier downwasting at Mt. Everest

In central Himalaya
Highest peak
Heavy debris-covered
Supra-glacial pond

Famous glaciers: Khumbu, Rongbuk, Ngozumpa, Kangxiong

Five acquisitions of bistatic TSX/TDX images, with long and short perpendicular baselines

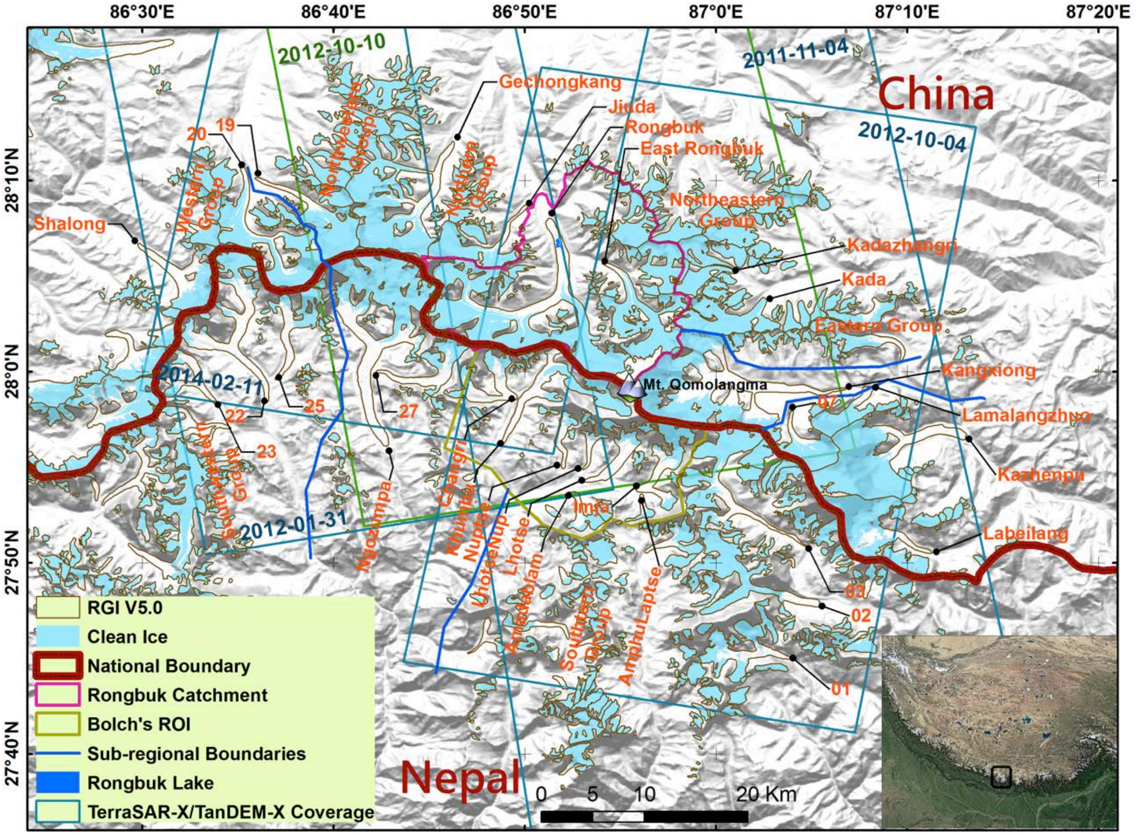

Heterogeneous pattern of glacier downwasting at Mt. Everest

Region or sub-region	Geodetic Glacier Mass Balance (m w.e. a^-1^)	Debris cover percentage
Total region	- 0.37 ± 0.13 (0.06)	17.7%
Chinese (Northern)	- 0.34 ± 0.13 (0.06)	15.3%
Nepalese (Southern)	- 0.41 ± 0.13 (0.06)	20.9%
Southeastern	- 0.28 ± 0.14 (0.09)	23.4%
Kangxiong	- 0.13 ± 0.14 (0.09)	27.0%
Northeastern	- 0.21 ± 0.14 (0.09)	3.7%
Rongbuk Catchment	- 0.51 ± 0.13 (0.07)	12.1%
Northwestern	- 0.19 ± 0.12 (0.05)	9.0%
Western	- 0.51 ± 0.12 (0.05)	31.6%
Ngozumpa	- 0.43 ± 0.12 (0.06)	36.7%
Bolch's	- 0.47 ± 0.14 (0.09)	47.2%

Errors in parentheses do not include component of penetration differences estimation.

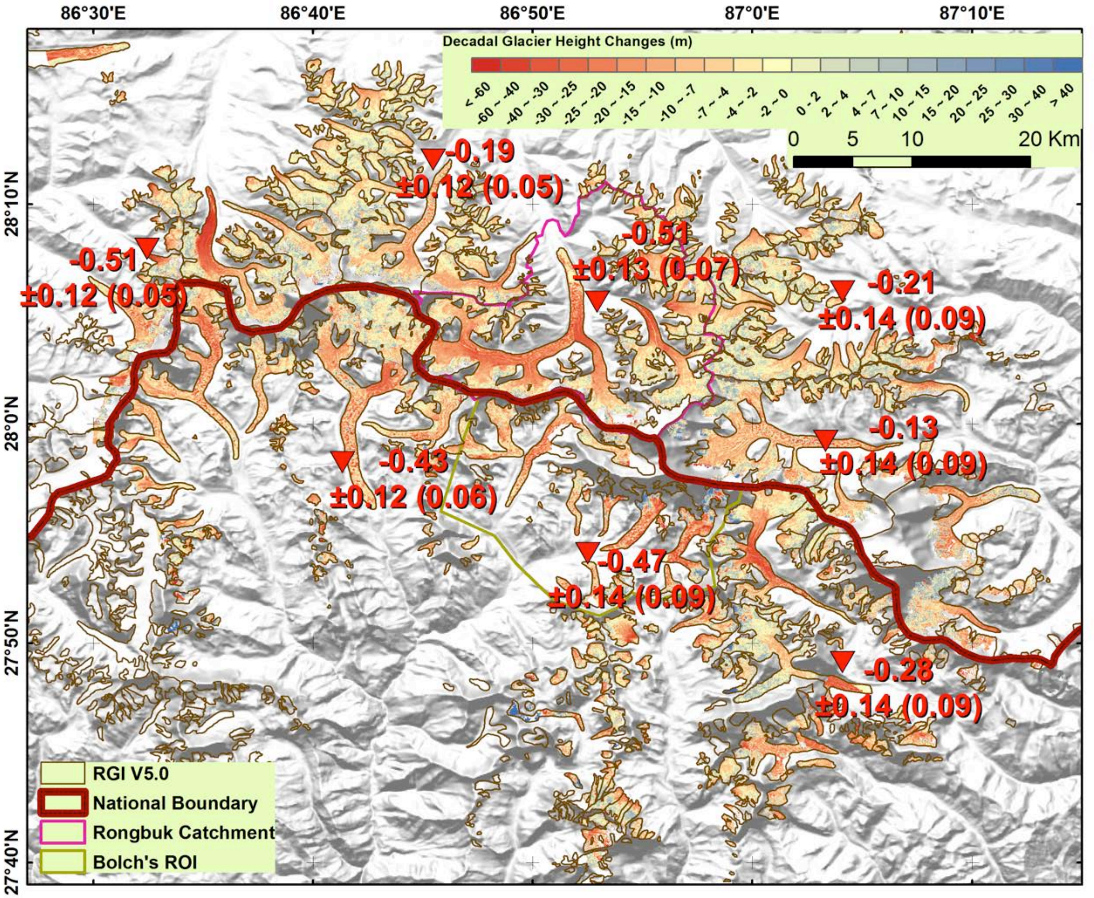

Heterogeneous pattern of glacier downwasting at Mt. Everest

Although in the Mt. Everest region, sub-regions with less debris-cover downwasted slower than those sub-regions with more debris; for one glacier, at same elevation level, usua debris still suppressed ice from melting in a warming trend.

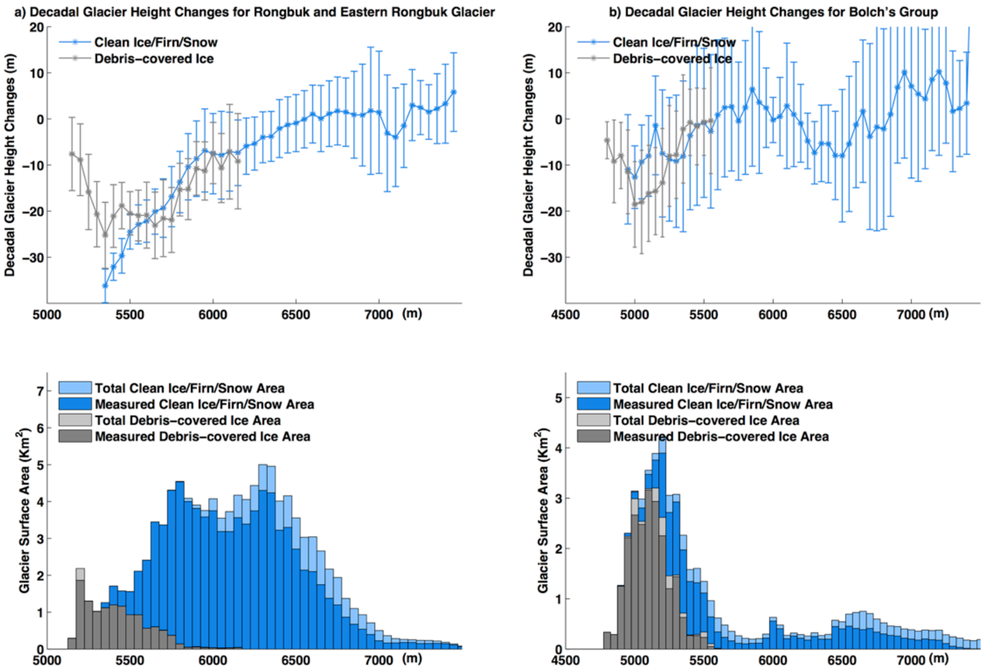

Ice cliffs close to rongbuk lake is dirty.

At downstream of ronbuk lake, no ice cliffs found for those supra-glacial ponds

Close to upper stream of rongbuk lake, ice cliffs and supra-glacial are very common, though ice-cliffs can hardly be identified from remote sensing images.

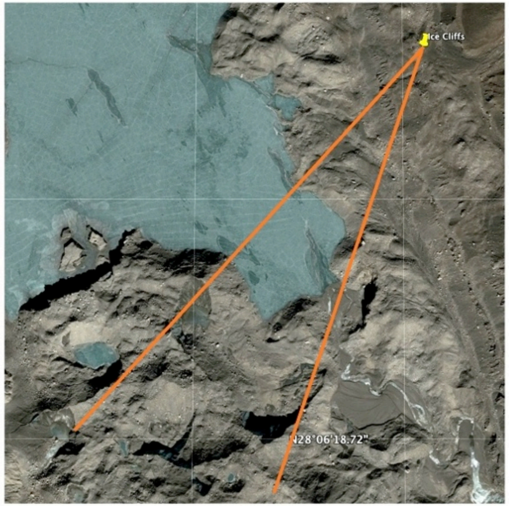

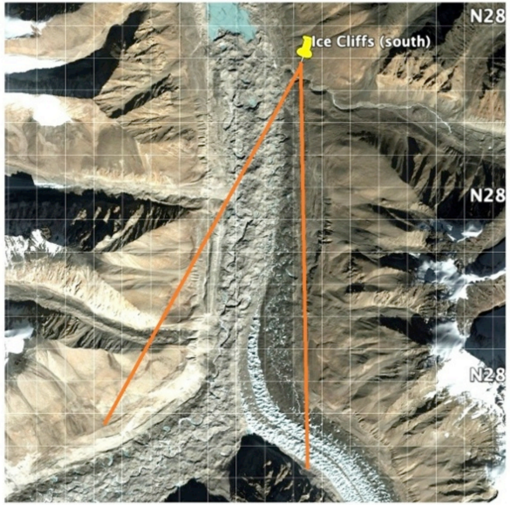

Heterogeneous pattern of glacier downwasting at Mt. Everest

Our derived results are consist with most previous studies in different sub-regions. After applying our estimated penetration, Gardelle et al.'s (2013TheCryo) result is quite similar to ours This suggested, at least in Mt. Everest, presuming X-band signal do not penetrate into snow/firn/ice surface is reasonable.

Rongbuk Catchment (Ye et al., 2015JHydro), and Khumbu surroundings (), records glacier mass balances since 1970s. Together with our observation, both region show glacier mass loss increasing. Increasing rate for Khumbu surroundings is greater than the north.

	GBM in other studies	GBM in this study
Rongbuk Catchment	-0.47 ± 0.23 (Ye et al., 1974-2006)	-0.53 ± 0.13 m w.e. a^{-1}
Bolch's ROI	-0.31 ± 0.08 (Bolch et al., 1970-2007)	-0.47 ± 0.14 m w.e. a^{-1}

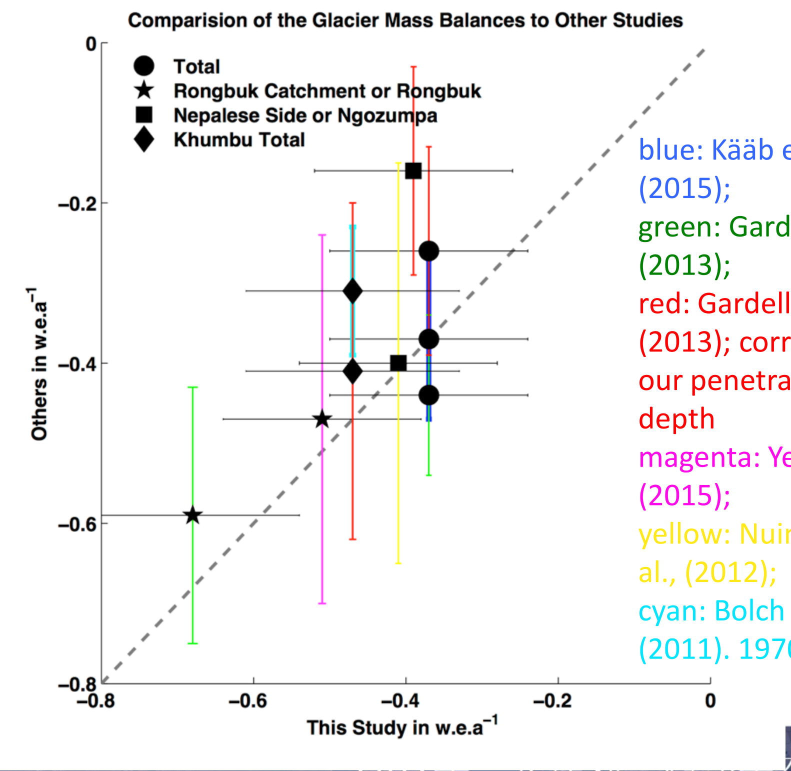

blue: Kääb et al., (2015);
green: Gardner et al., (2013);
red: Gardelle et al., (2013); correct to our penetration depth
magenta: Ye et al., (2015);
yellow: Nuimura et al., (2012);
cyan: Bolch et al., (2011). 1970-2007

Principle of bistatic interferometry

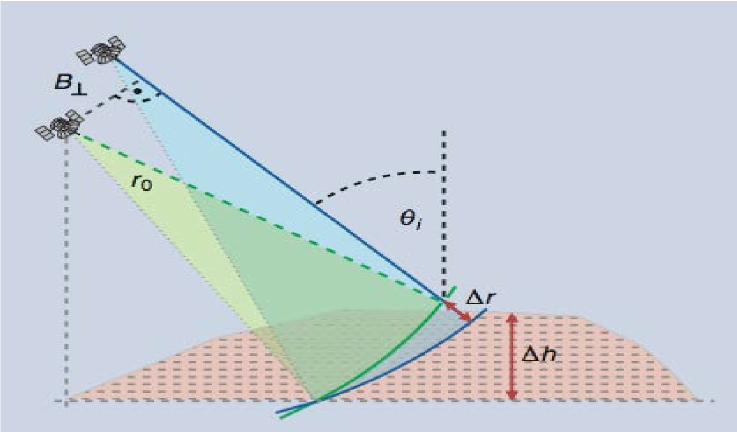

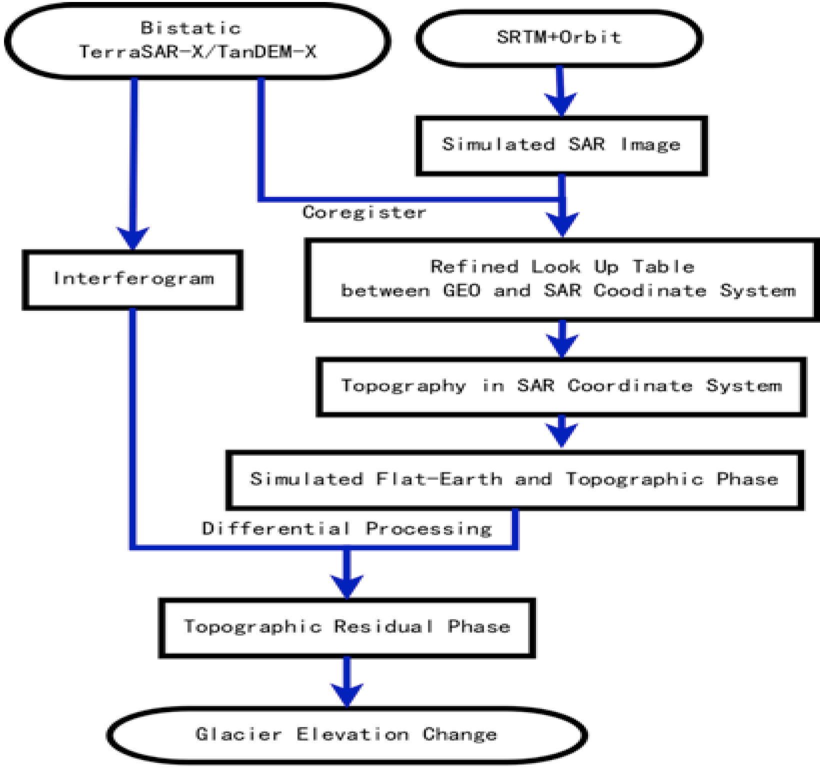

Directly transferring topographic residual phase can reduce unwrapping error to some extent.

$$\Delta\varphi_{bi} = \Delta\varphi_{flat\_bi} + \boxed{\Delta\varphi_{height\_bi}} = -\frac{2\pi B_\perp r}{\lambda R \tan\theta} - \frac{2\pi B_\perp \Delta h}{\lambda R sin\theta} \quad (1)$$

$$\Delta\varphi_{height\_bi} = -\left(\frac{2\pi B_\perp \Delta h_{srtm}}{\lambda R sin\theta} + \frac{2\pi B_\perp \Delta h_{residual}}{\lambda R sin\theta}\right) \quad (2)$$

where $B_\perp$ is perpendicular baseline, λ is wave length, θ incidence angle, r is horizontal distance between two points on the earth and R is slant range distance. Δh is height, which can be diveded into height in SRTM DEM (Δh_{srtm}) and height change ($\Delta h_{residual}$) due to glacier thickening or thinning.

Post processing after Bistatic D-InSAR

Penetration depths were corrected in each 50m elevation bins and separately for clean-ice and debris-cover glacier.

Foreshortening region were identified with TSX/TDX orbital information and DEM (slope and aspect) information and masked out.

SRTM void regions were masked out.

Unwrapping error regions were masked out.

TSX/TDX orbital ramp were corrected with quadratic polynomial regression to off-glacier region by presuming no deformation occurred at off-glacier region between 2000 and when TSX/TDX images obtained.

Post processing after Bistatic D-InSAR

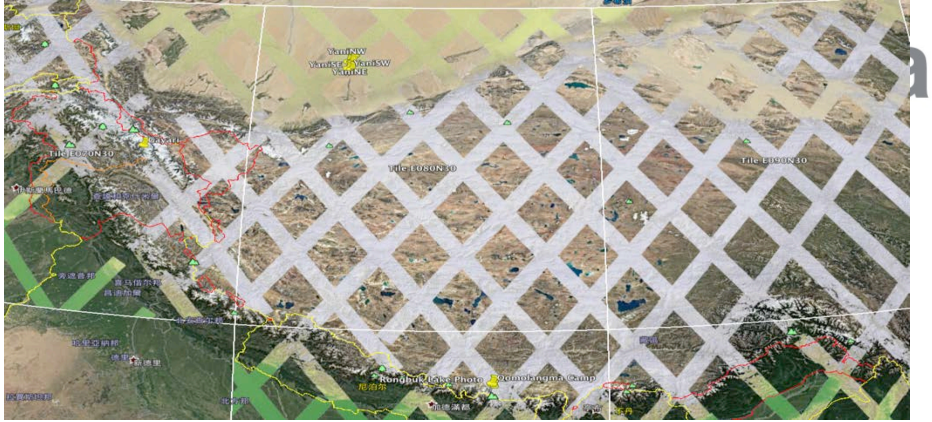

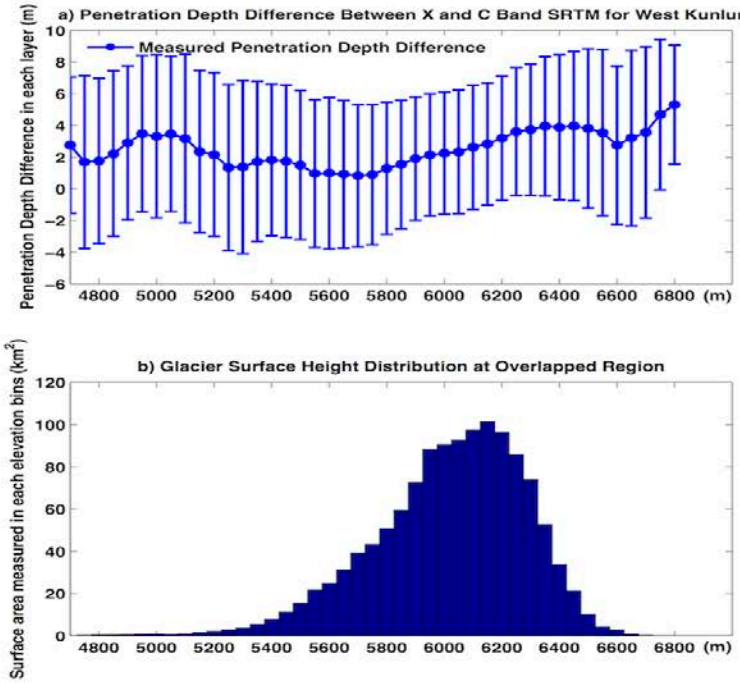

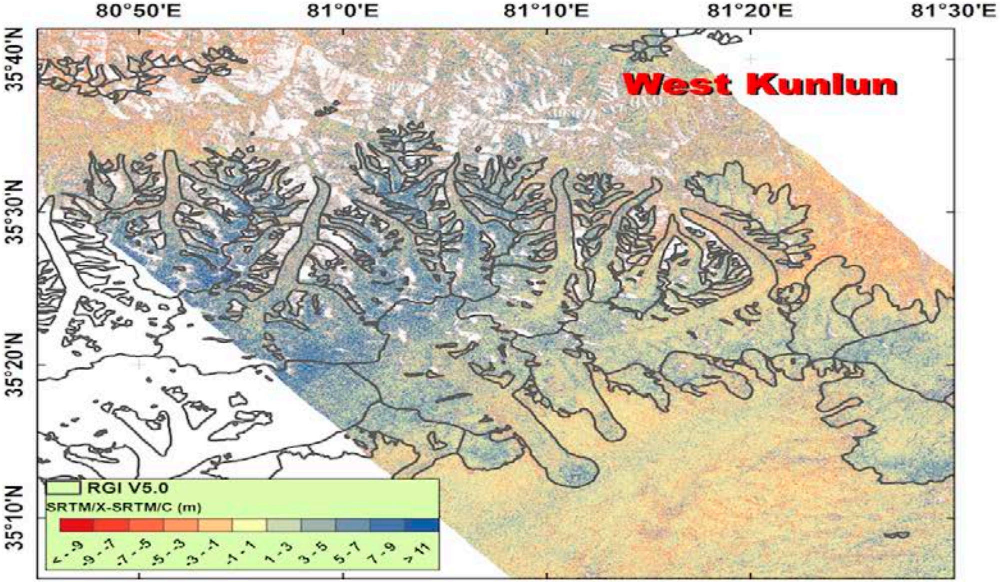

Post processing after Bistatic D-InSAR

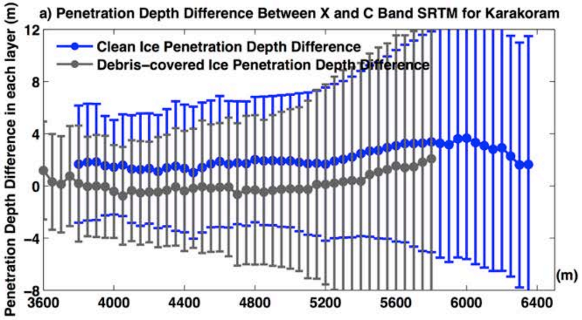

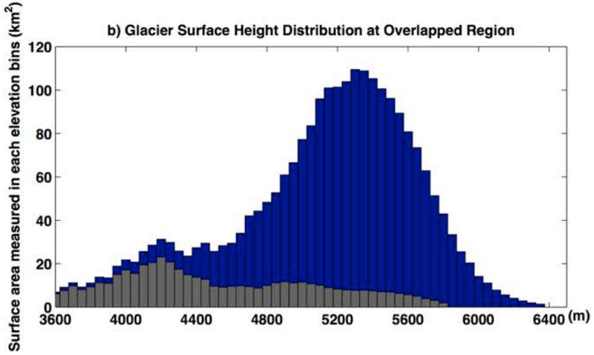

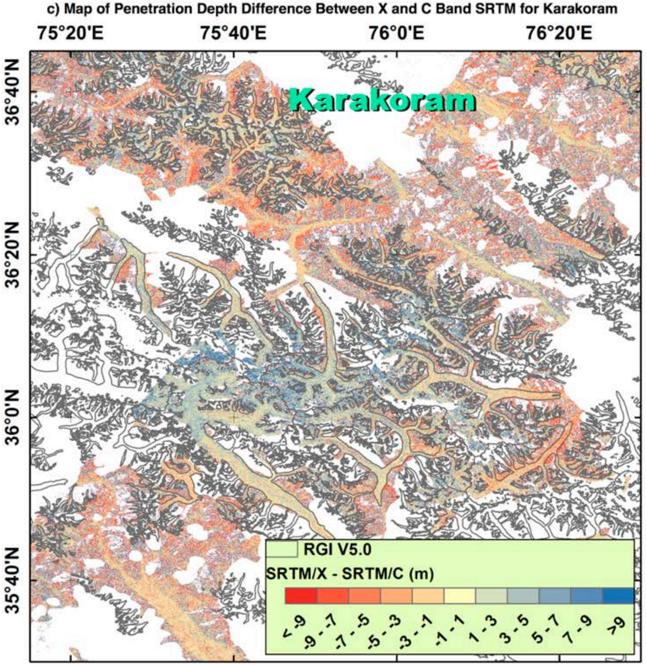

Post processing after Bistatic D-InSAR

In westerlie dominated region, penetration differences are deeper at upperstream, while at monsoon dominated region penetration depth are almost the same that all elevation bins.

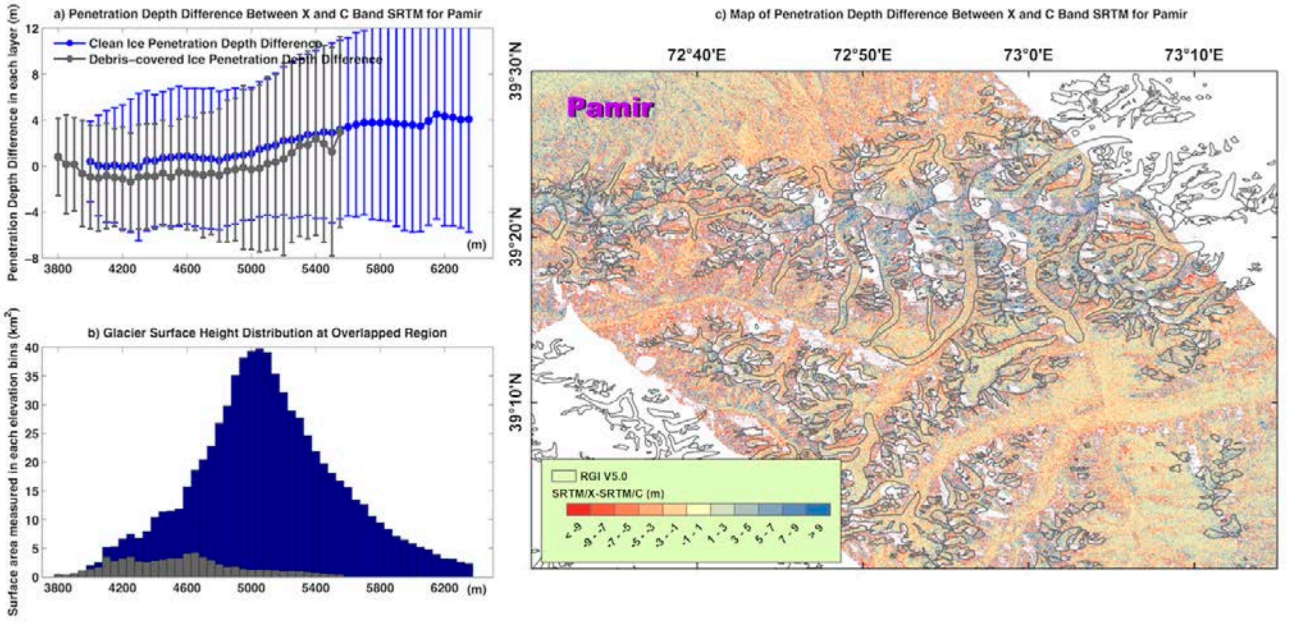

Post processing after Bistatic D-InSAR

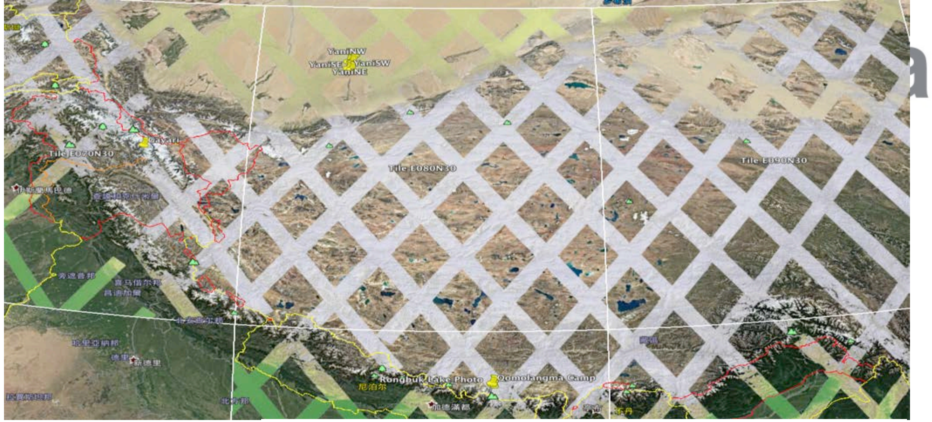

Datum differences between different orbital coverage

Corrected

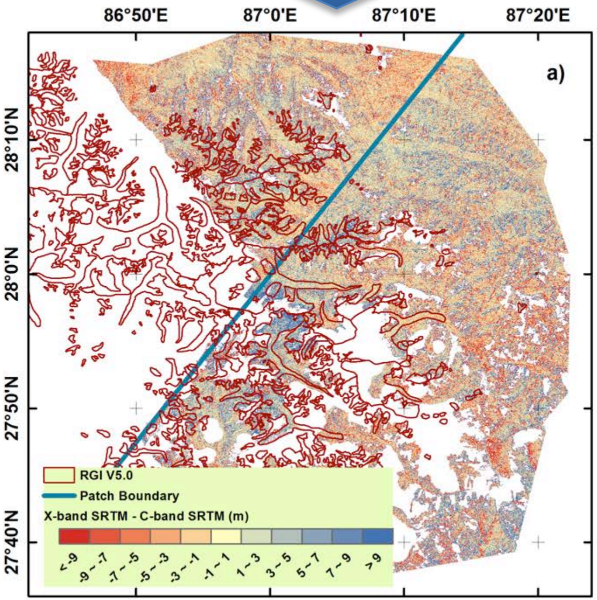

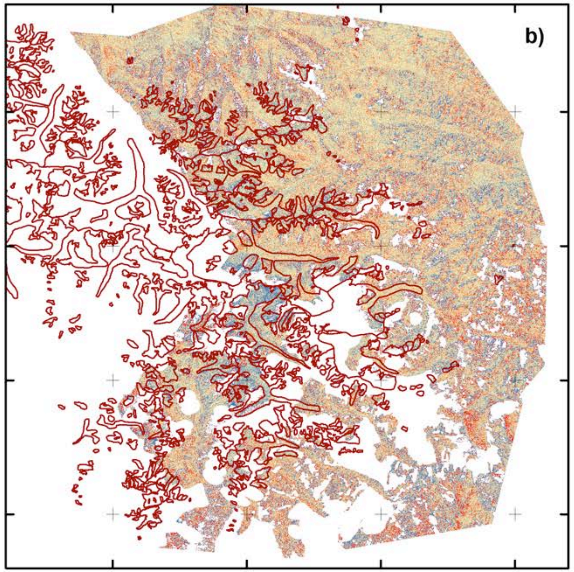

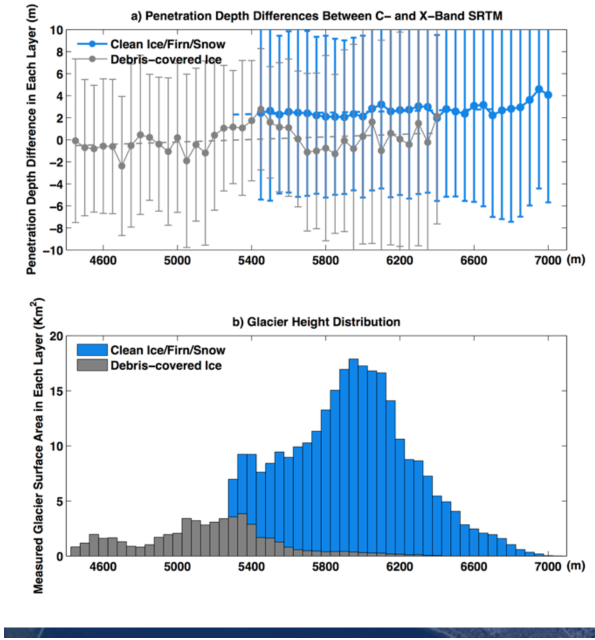

Post processing after Bistatic D-InSAR

Penetration depths were corrected in each 50m elevation bins and separately for clean-ice and debris-cover glacier.

Foreshortening region were identified with TSX/TDX orbital information and DEM (slope and aspect) information and masked out.

SRTM void regions were masked out.

Unwrapping error regions were masked out.

TSX/TDX orbital ramp were corrected with quadratic polynomial regression to off-glacier region by presuming no deformation occurred at off-glacier region between 2000 and when TSX/TDX images obtained.

Post processing after Bistatic D-InSAR

$$\theta_{local} = \theta_{flat} + \text{Slope} * \sin(\text{Aspect} - \text{Heading})$$

θ_{local} is the local incidence angle, and θ_{flat} is the incidence angle on flat terrain. The heading is the orbital azimuth direction with respect to north, which is approximately 191° for descending images and -9° for ascending images.

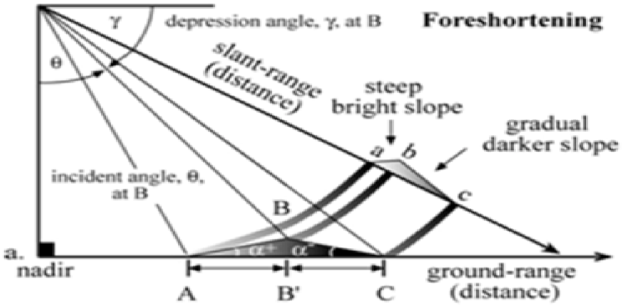

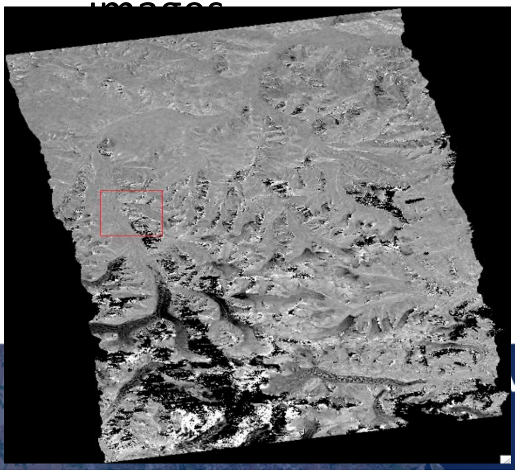

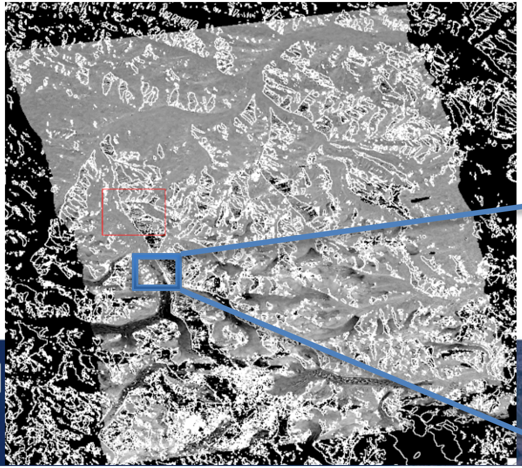

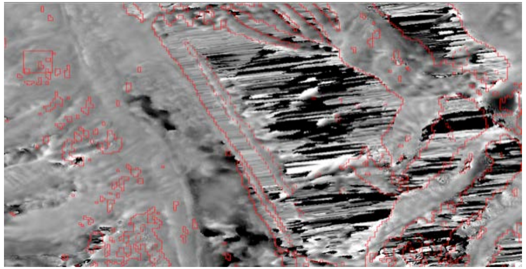

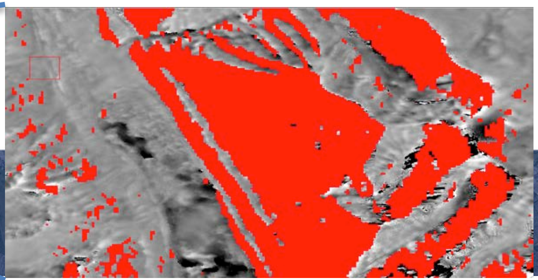

学术研讨会

，丹麦 哥本哈根

Post processing after Bistatic D-InSAR

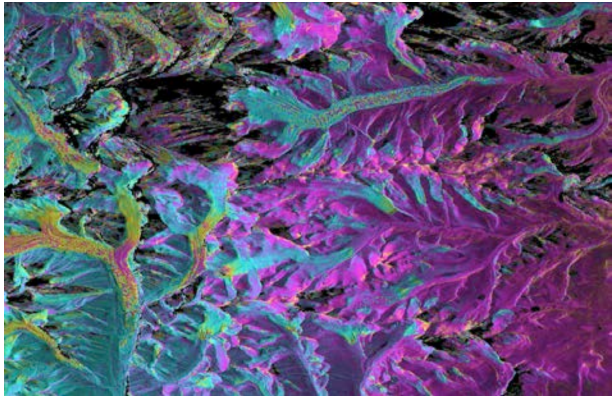

geocoding

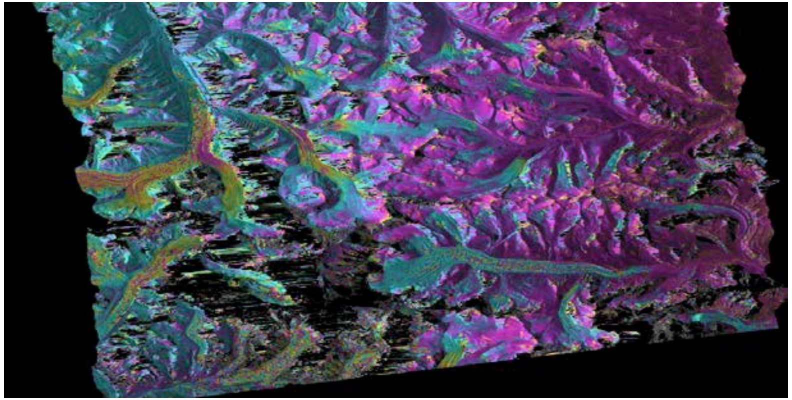

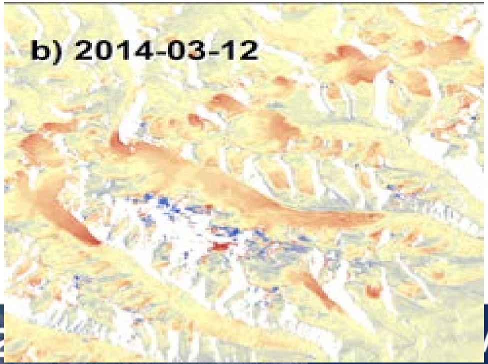

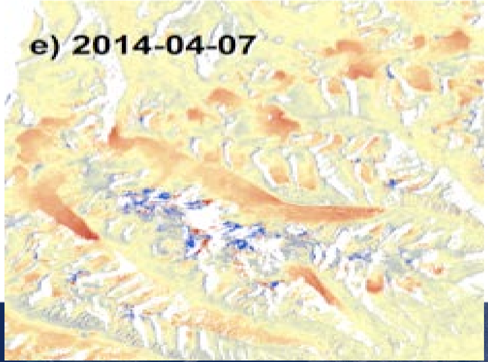

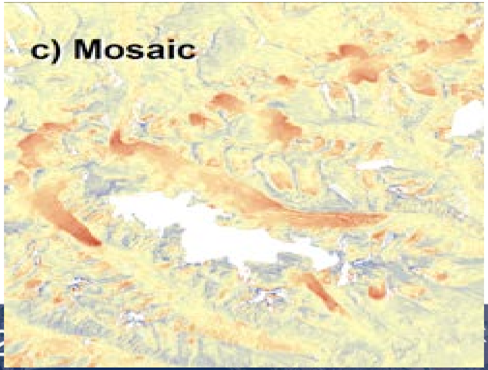

Ascending

Descending

Multi perpendicular baseline

Longer the perpendicular baseline is, the higher gradient of phase is, leading to unwrapping error

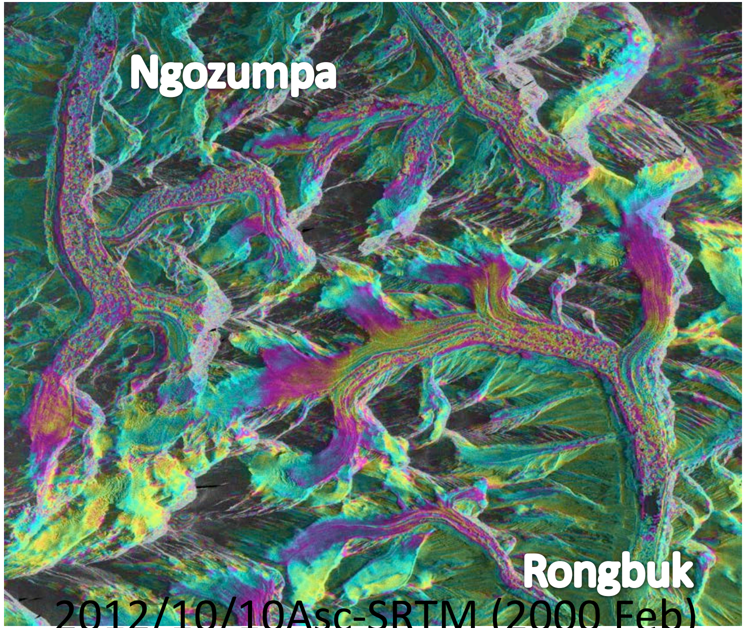

2012/10/10Asc-SRTM (2000 Feb)
Bn=391m Height Ambiguity=-28m

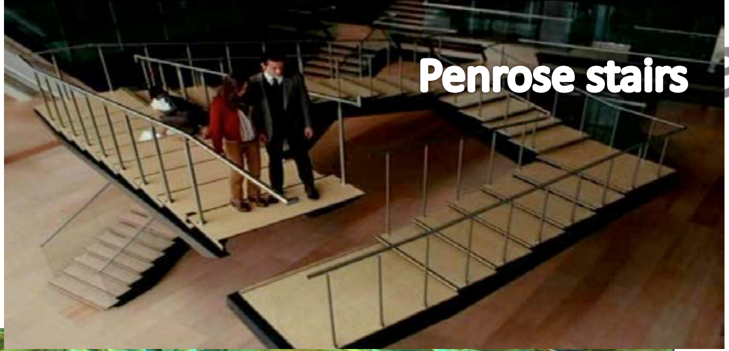

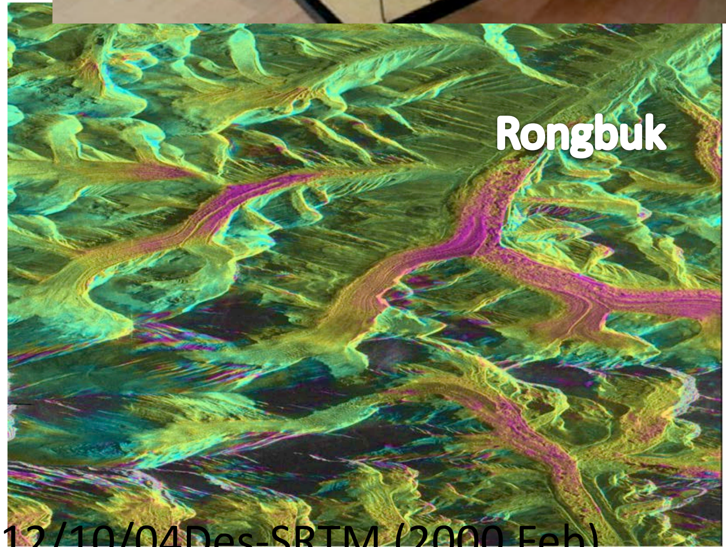

2012/10/04Des-SRTM (2000 Feb)
Bn=176.2m Height Ambiguity=71.5m

Acquisition Date	Orbital Number	Pass	Effective Baseline	Height Ambiguity (m)	Master Satellite
2011-11-04	128	Ascending	113.8	-49.9	TSX
2012-01-03	128	Ascending	83.2	-62.9	TSX
2012-10-04	29	Descending	88.1	71.5	TSX
2012-10-10	128	Ascending	195.5	-28.0	TSX
2014-02-11	29	Descending	126.2	53.8	TSX

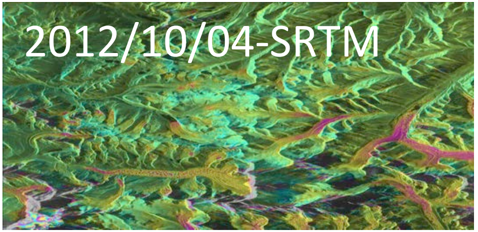

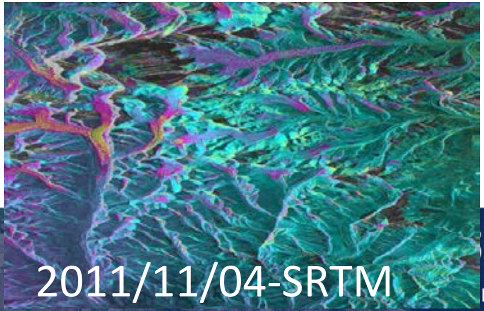

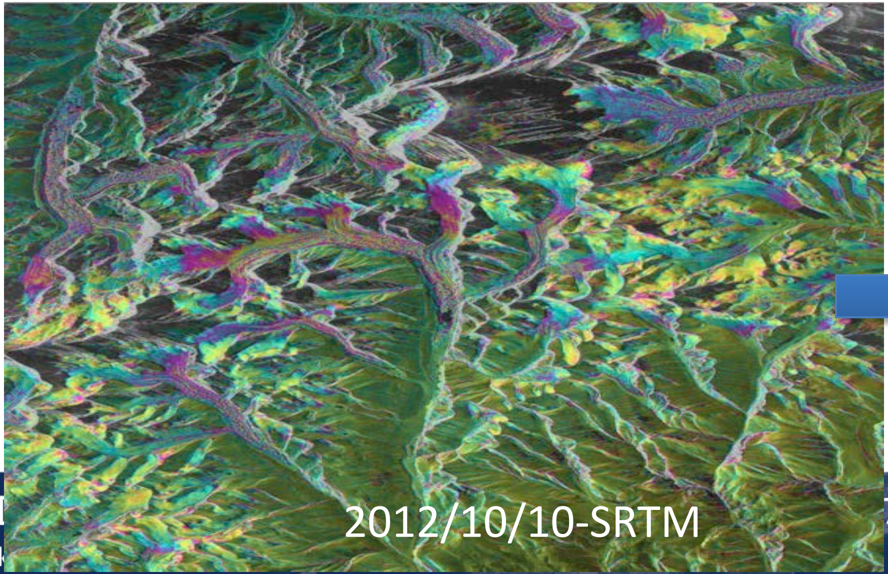

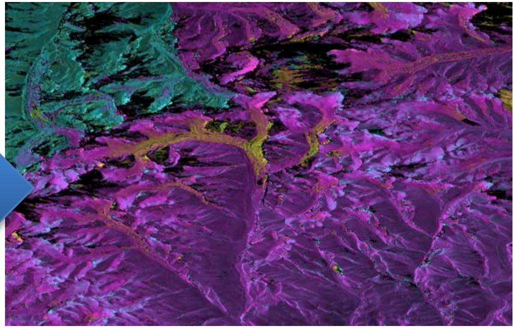

2012/10/10-SRTM
Unwrapping error

The DEM output in each iteration will be regarded as reference in next iteration of DInSAR

Iteration 1 | Iteration 2 | Iteration 3

04 20 12 / 10 /

10 20 12 / 10 /

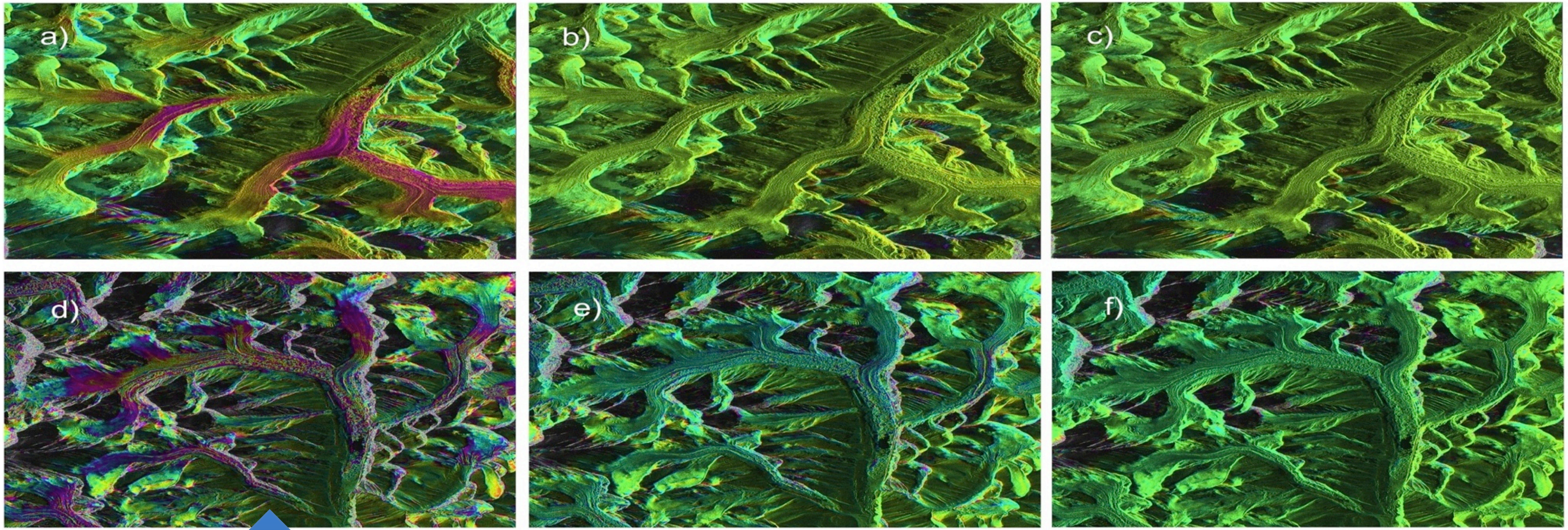

not participate in the first iteration

Accuracy Estimation

Glacier height changes

Error

- **Random Part**: $$\frac{Err_{bi-SRTM}}{\sqrt{Neff_{bi-SRTM(On)}}}$$
- **Systematic**: $$Err_{sys} = \sqrt{Err_{pd}^{2} + Err_{Mon}^{2} + Err_{datum}^{2}}$$
  - **Seasonal**
  - **Datum**: $$\frac{Err_{bi-SRTM}}{\sqrt{Neff_{bi-SRTM(Off)}}}$$
  - **Penetration Depth**
    - **Random**: $$\frac{Err_{cx\_on}}{\sqrt{Neff_{cx\_on}}}$$
    - **Systematic (Datum)**: $$\frac{Err_{cx\_off}}{\sqrt{Neff_{cx\_off}}}$$

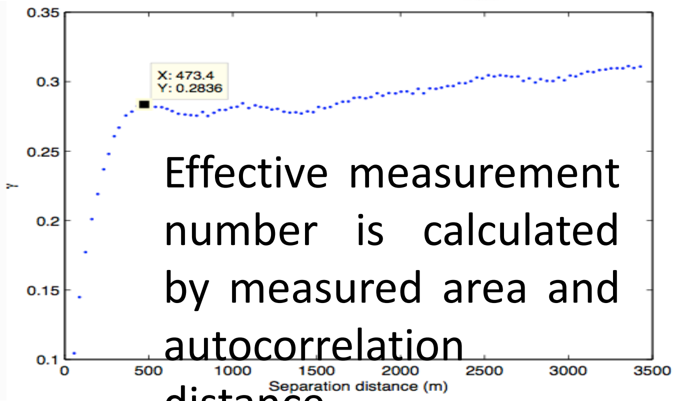

Effective measurement number is calculated by measured area and autocorrelation distance.

$N_{eff}=Area/(Dist_{Ac}^{2})$

Study site and Data

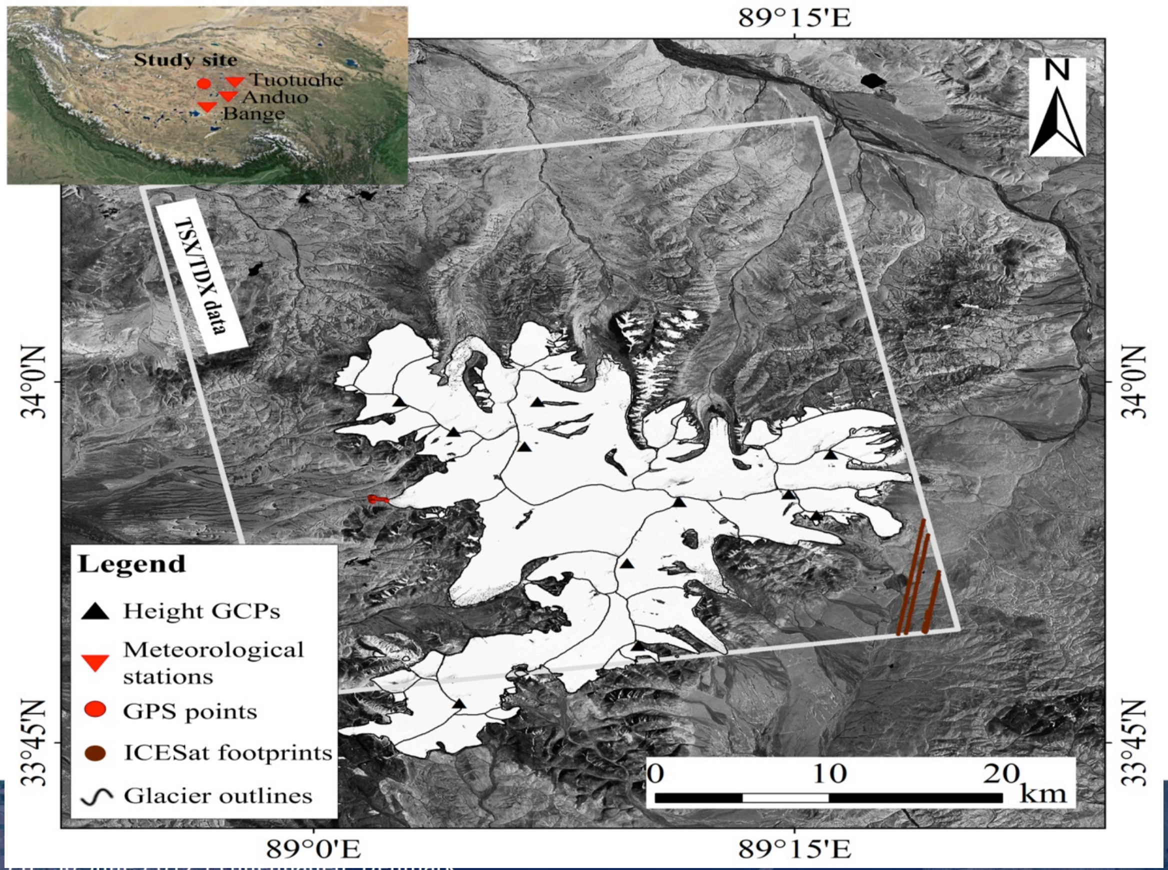

(1) Two TanDEM-X bistatic SAR数, obtained on 2012.1.26和2016.1.28

(2) Height elevation：GCP、GPS、ICESat；

(3) SRTM-C DEM in 30m；

(4) Landsat optical data；

Glacier Elevation Changes (2012-2016)

(1) 2012-2016 glacier height changes for Puruogangri: **-1.27±0.11 m** (-0.317±0.027 m yr^{-1})

(2) Slight height increasing in centre of the ice field; terminal downwasted at different rate。

(3) **5Z213E0012** increased at it terminal， upper part downwasted。

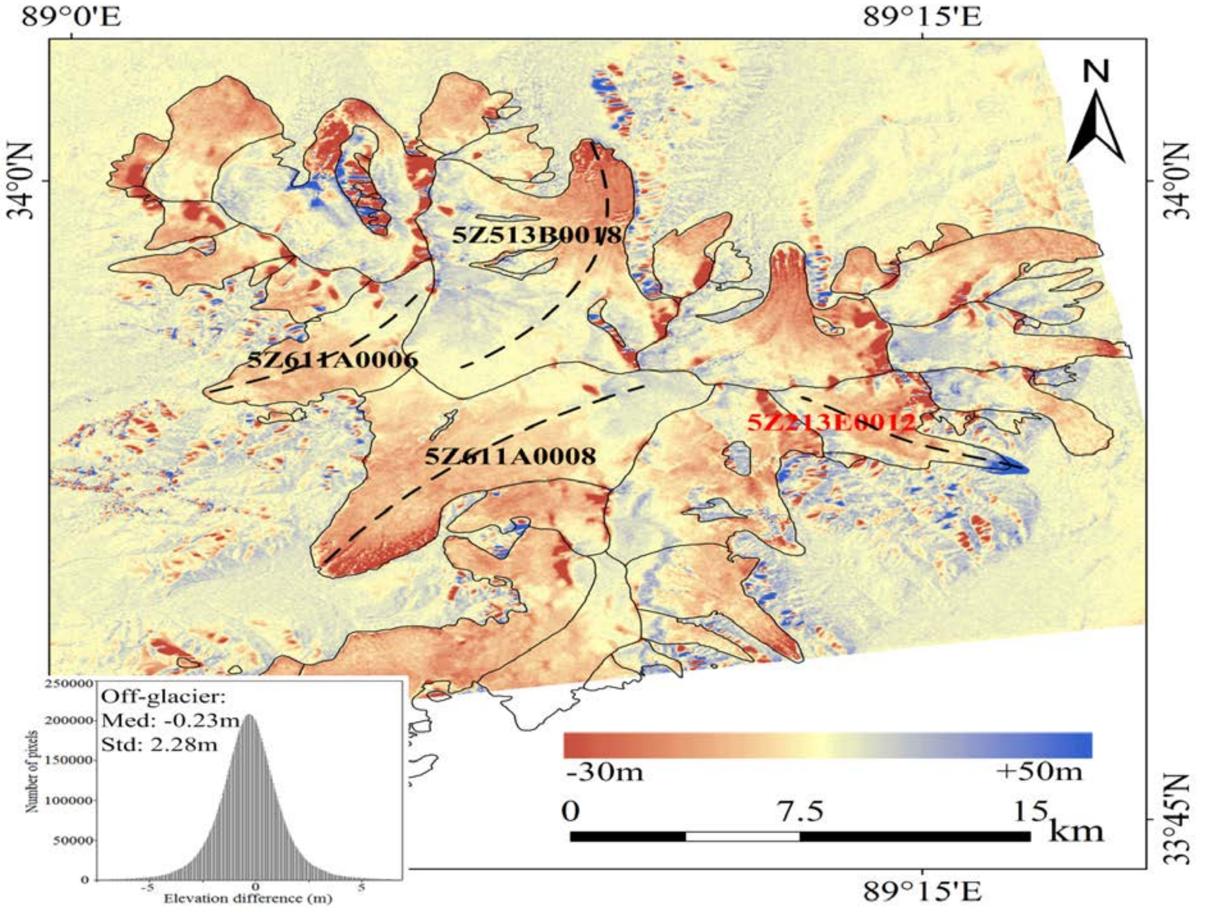

Multi period：2000-2012 Vs. 2012-2016

period	Mass balance	Study
1974-2000年	-0.238±0.073 m yr^{-1}	Lei et al., (2012)
2000-2012年	-0.049±0.200 m yr^{-1}	Neckel et al., (2013)
2012-2016年	-0.317±0.027 m yr^{-1}	This study

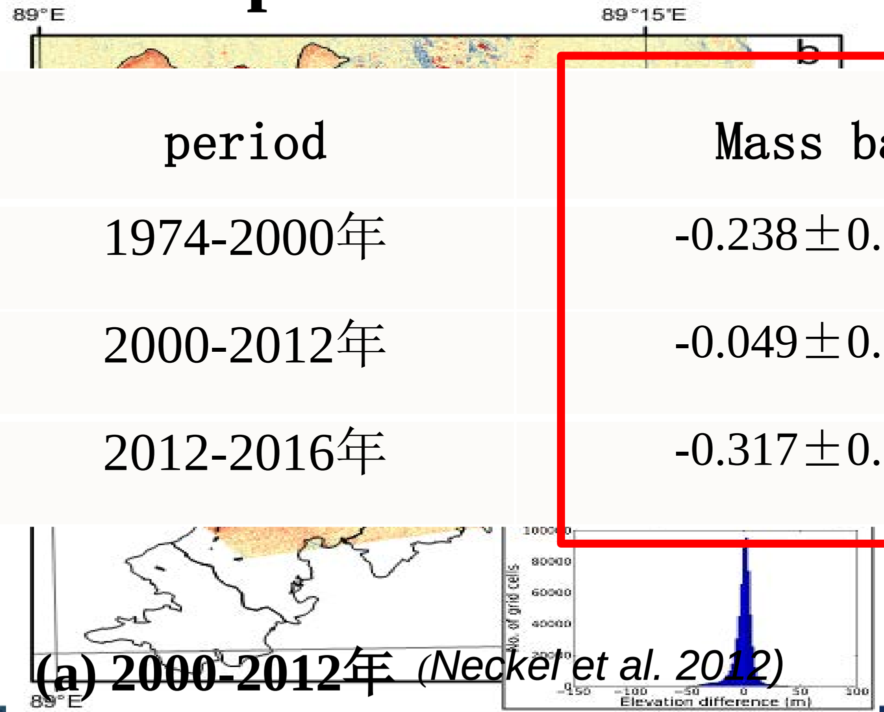

(a) 2000-2012年 *(Neckel et al. 2012)*

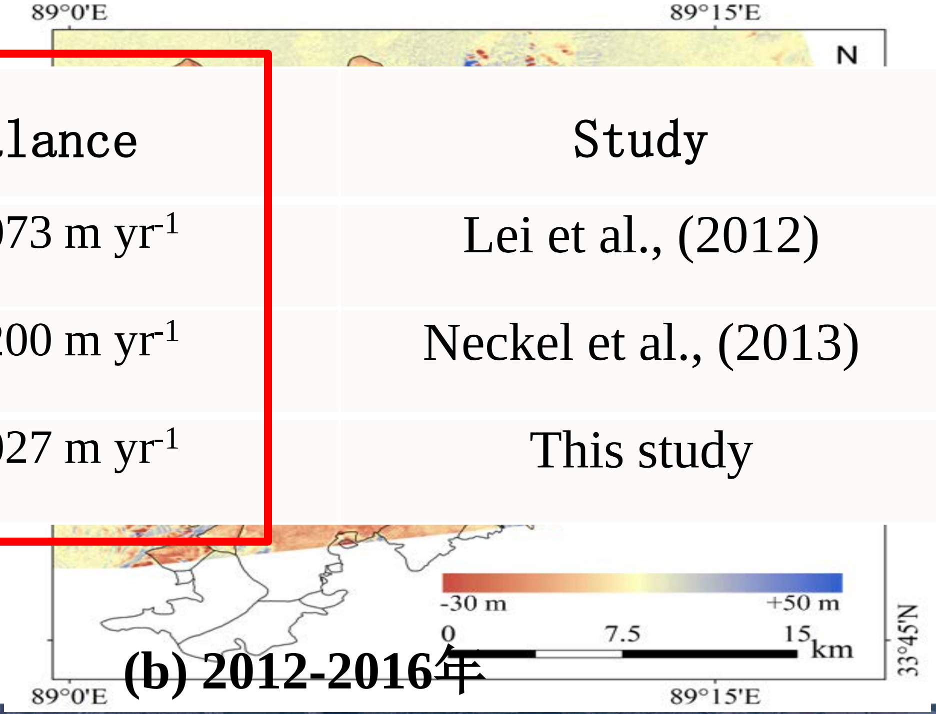

(b) 2012-2016年

Glacier elevation changes & climate change

(1) Since 1974, as temperature in JJL kept increasing, **Puruogangri Ice Field continued downwasted .**

(2) Glacier mass balance are different in three period; which could be due to precipitation differences. Precipitation during 2000-2012 are most, 2012-2016 are less, and 1980-2000 are the least.

(3) After 2010, the Puruogangri Ice Field downwasted rate significantly increasing, which could be due to both temperature increasing and precipitation decreasing.

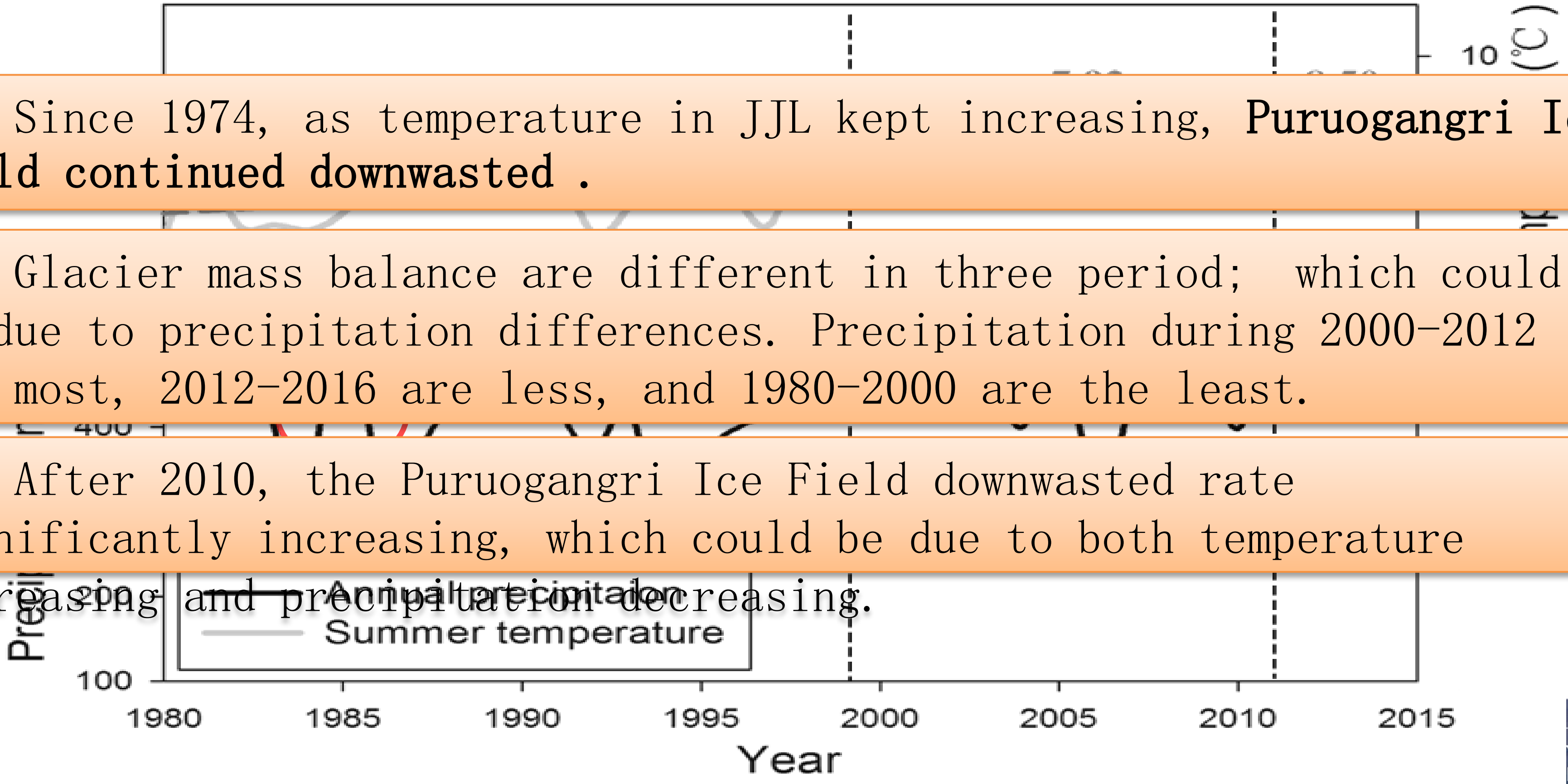

Glacier elevation changes & local factors

Correlations between glacier mass balance and individual morphometric factors

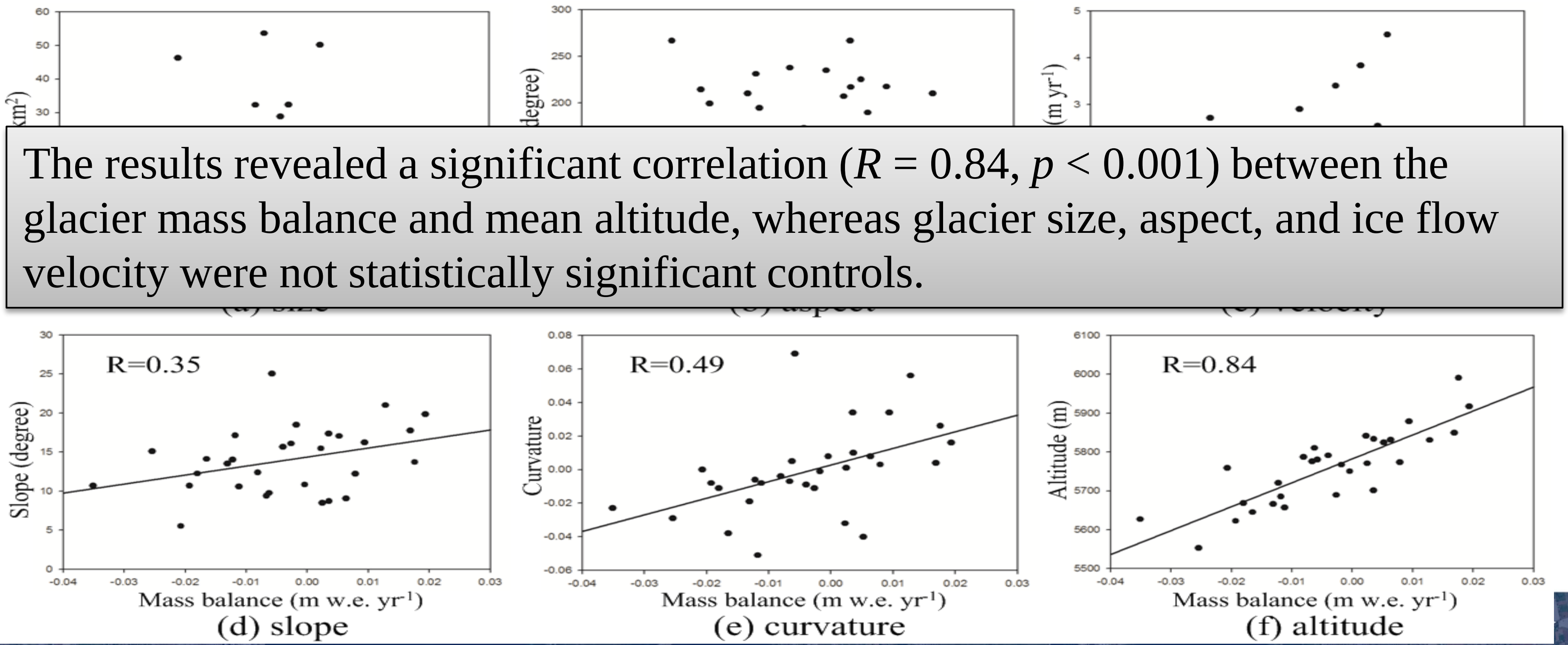

The results revealed a significant correlation ($R = 0.84$, $p < 0.001$) between the glacier mass balance and mean altitude, whereas glacier size, aspect, and ice flow velocity were not statistically significant controls.

Glacier elevation changes & morphometric factors

Correlations between elevation changes and morphometric factors at local scale (grid size of 10×10 pixels)

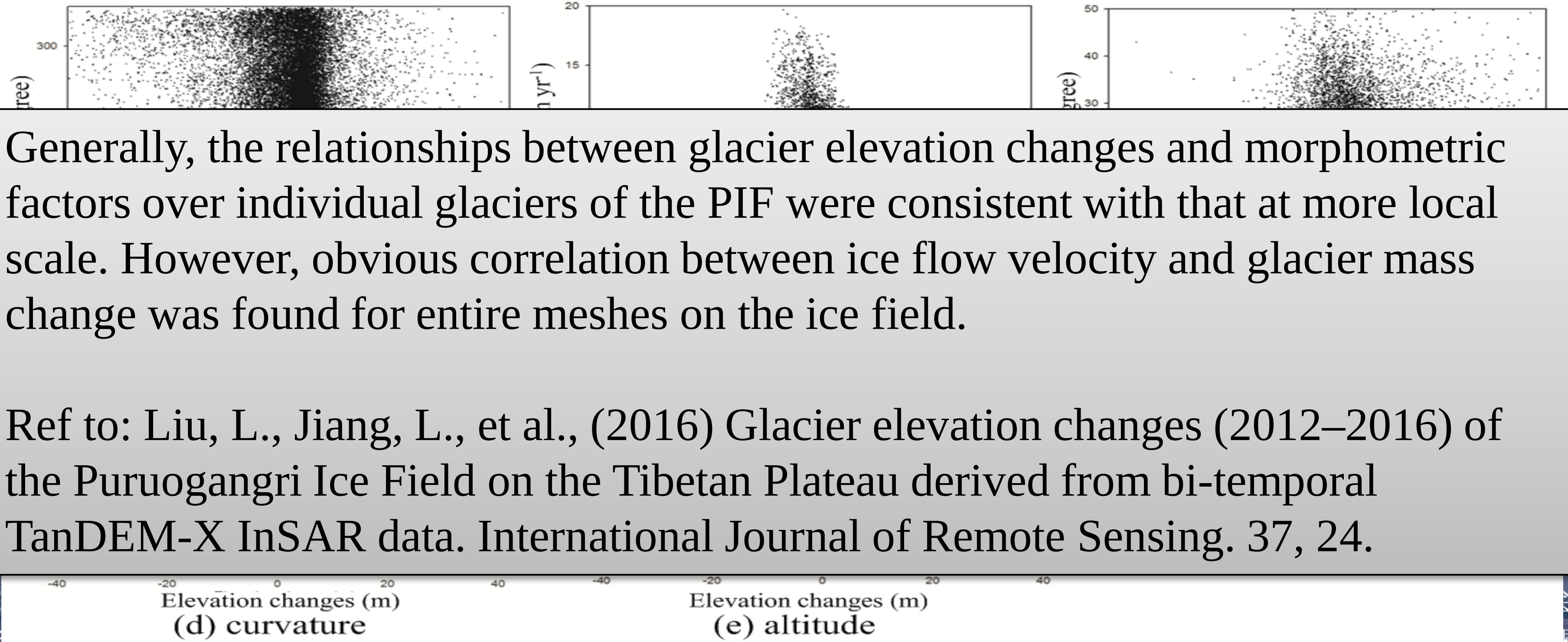

Generally, the relationships between glacier elevation changes and morphometric factors over individual glaciers of the PIF were consistent with that at more local scale. However, obvious correlation between ice flow velocity and glacier mass change was found for entire meshes on the ice field.

Ref to: Liu, L., Jiang, L., et al., (2016) Glacier elevation changes (2012–2016) of the Puruogangri Ice Field on the Tibetan Plateau derived from bi-temporal TanDEM-X InSAR data. International Journal of Remote Sensing. 37, 24.

The Chinese University of Hong Kong

The University of Leeds